

# Quasi-local black hole horizons

Badri Krishnan

*Max Planck Institute for Gravitational Physics (Albert Einstein Institute),  
Callinstr. 38, 30167 Hannover, Germany*

October 11, 2018

## Abstract

This article introduces the subject of quasi-local horizons at a level suitable for physics graduate students who have taken a first course on general relativity. It reviews properties of trapped surfaces and trapped regions in some simple examples, general properties of trapped surfaces including their stability properties, the definitions and some applications of dynamical-, trapping-, and isolated-horizons.

## 1 Introduction

The first conception of a black hole was due to Michell and Laplace in the 18<sup>th</sup> century. They viewed it as a star whose gravitational field is so strong that the Newtonian escape velocity  $\sqrt{2GM/R}$  (with  $M$  and  $R$  being the mass and radius of the star respectively) is larger than the speed of light. The condition on the escape velocity leads to the inequality  $R \leq 2GM/c^2$  which, remarkably, also holds in general relativity. While such a star would have the property that not even light can escape from it, this is however a non-relativistic concept. The speed of light is not privileged in pre-relativistic physics, and a moving observer would not necessarily see it as a dark object. A more complete account of this history is given by Hawking and Ellis [39] including reprints of the original articles.

The history of black holes proper dates back to just after the discovery of general relativity. The first non-trivial exact solution to the Einstein equations discovered by Schwarzschild in 1916 and named after him was, in fact, a black hole. It was however more than four decades before its properties were fully appreciated. The Kruskal-Szekeres extension of the Schwarzschild solution was discovered only in 1960. This was shortly followed by the discovery of the Kerr solution in 1963 representing spinning black holes. Its global properties were explained by Carter in 1966. The Kerr-Newman solution representing charged, spinning black holes was discovered in 1965. It was in 1964 that the phrase “black hole” was first coined by John Wheeler. During the same time, there were seminal developments in understanding the general properties of black holes beyond specific examples. This includes the study of the global properties of black hole spacetimes, the definition of event horizons, and crucially for the developments to be discussed here, the singularity theorems of Penrose and Hawking and the introduction of trapped surfaces by Penrose. This was soon followed by the understanding of black hole thermodynamics by Bekenstein, Bardeen, Carter and Hawking in 1973, and the discovery of Hawking radiation in 1974. The cosmic censorship hypothesis was formulated by

Penrose in 1979. The question of whether this is valid, i.e. if every singularity that results from the future evolution of generic, regular initial conditions is hidden behind an event horizon, is not settled and is one of the key unsolved questions in classical general relativity. The black hole uniqueness theorems which showed that the Kerr-Newman solutions are the unique globally stationary black hole solutions in Einstein-Maxwell theory in four dimensions was established in the 1980s following the work of Israel, Carter and Robinson.

More recently, black holes have been the subject of intense study in quantum gravity where the calculation of black hole entropy has been seen as a key milestone for string theory and loop quantum gravity. There have also been important developments on the classical side where the long standing problem of calculating the gravitational wave signal from the merger of two black holes was finally solved numerically in 2005 by Pretorius. In an astrophysical context, black holes are believed to be engines for some of the most violent events in our universe, such as active galactic nuclei. Astronomers have succeeded in locating a large number of black hole candidates with masses ranging from a few to billions of solar masses, and the direct detection of gravitational waves from binary black hole systems is expected later this decade.

Most of these seminal developments have relied on event horizons to characterize the boundary of the black hole region (the singularity theorems are a notable exception). This is completely reasonable when we are dealing with stationary situations, but can lead us astray in dynamical situations. As we shall elaborate later, event horizons are global notions and it is in principle not possible for a mortal observer to locate them. One possible alternative is to use the notion of trapped surfaces introduced by Penrose. While not entirely local since they are closed spacelike surfaces, these provide a quasi-local alternative which an observer could in principle locate in order to detect the presence of a black hole. Trapped surfaces lead logically to various kinds of quasi-local horizons including isolated, dynamical and trapping horizons. The goal of this chapter is to motivate and explain the quasi-local approach to studying black hole horizons, and to review some recent results. Somewhat surprisingly, we shall see there is still a major gap in our understanding of classical black holes in dynamical spacetimes. If we accept black holes as bonafide astrophysical objects, we still do not have a satisfactory notion of what the surface of a black hole is. Event horizons are not satisfactory because of their global properties, but there is as yet no established quasi-local alternative.

The style of this chapter will typically be to start informally with simple examples and to use them as guidance for developing general concepts and definitions. In Sec. 2 we shall start with the simplest black hole, i.e. the spherically symmetric Schwarzschild spacetime, and understand the properties of its black hole region. This naturally motivates the fundamental notions of event horizons and trapped surfaces, and to the boundary of the trapped region. As we shall see, the different reasonable definitions of the black hole horizon agree in Schwarzschild. This will not be the case in more general situations. Perhaps the simplest example is the imploding Vaidya spacetime which shall be our second example in Sec. 2.2. We shall see that at least in this simple spherically symmetric example, the location of the trapped surfaces can be determined. These two examples are then followed by general definitions of event horizons, and trapped surfaces in Sec. 3 which formalizes many notions introduced in Sec. 2. Some properties of trapped surfaces under deformations and time evolution are then discussed in Sec. 3.3, and this leads naturally to the notions of marginally trapped tubes, and trapping and dynamical horizons. We then restrict our attention to isolated horizons which describes the equilibrium case, when no matter or radiation is falling into the black hole (but the rest of spacetime is allowed to be dynamical). This is now well understood and we review the general formalism in Sec. 4 with the Kerr black hole as the prototypical example. In particular, we discuss two applications: black hole thermodynamics and the spacetime in the neighborhood of an isolated black hole. Sec. 5 reviews some results and applications for dynamical horizons and finally Sec. 6 provides a summary and some open issues.

The discussion of this chapter will be mostly self-contained, though digressions into the relevant mathematical concepts will be necessarily brief. Useful references for black holes and general relativity are [26, 65], and for more mathematically inclined readers [50] is recommended as a useful introduction to the relevant concepts in differential geometry. The discussion is meant to be accessible to physics graduate students who have taken a first course in general relativity (covering, say, the first part of the textbook by Wald [65]). In the same spirit, the list of references is not meant to be exhaustive in any sense, and is mostly biased towards reviews and pedagogical material. The selection of topics is not meant to be exhaustive; this contribution is *not* to be viewed as a broad review article. It is rather a combination of pedagogically useful examples, and a brief description of some recent results. This material will hopefully whet the reader's appetite and motivate him/her to delve further into the subject.

Some words on notation are in order. A *spacetime* is a smooth four-dimensional manifold  $\mathcal{M}$  with a Lorentzian metric  $g_{ab}$  with signature  $(-+++)$ . We shall use a combination of index-free notation and Penrose's abstract index notation for tensors [56]; lower-case Latin letters  $a, b, c, \dots$  will denote spacetime indices. Symmetrization of indices will be denoted by round brackets, e.g.  $X_{(ab)} := (X_{ab} + X_{ba})/2$ , and anti-symmetrization by square brackets:  $X_{[ab]} := (X_{ab} - X_{ba})/2$ . The derivative-operator compatible with  $g_{ab}$  will be denoted  $\nabla_a$ , and the Riemann tensor  $R_{abcd}$  will be defined by  $2\nabla_{[a}\nabla_{b]}X_c = R_{abc}{}^d X_d$  for an arbitrary 1-form  $X_a$ . The Ricci tensor and scalar are respectively  $R_{ab} = R_{acb}{}^c$  and  $R = g^{ab}R_{ab}$ . The coordinate derivative operator will be denoted  $\partial$ . The exterior derivative will be either denoted by indices, such as  $\nabla_{[a}X_{b]}$ , or in index free notation as  $dX$ . The Lie derivative of an arbitrary tensor field  $T$  along a vector field  $X$  will be denoted  $\mathcal{L}_X T$ . Where no confusion is likely to arise, we shall often not explicitly include the indices in geometric quantities. Unless otherwise mentioned, we shall work in geometrical units with  $G = 1$  and  $c = 1$ . We shall often deal with sub-manifolds of  $\mathcal{M}$ ; a sub-manifold of unit co-dimension will be called a hyper-surface while lower dimensional manifolds (typically these will be 2-spheres topologically) will be called surfaces. All sub-manifolds shall be assumed to be sufficiently smooth. Unless mentioned otherwise, we shall be working with standard general relativity in four spacetime dimensions.

## 2 Simple examples

### 2.1 The trapped region in Schwarzschild spacetime

We shall start by studying the gravitational field in the vicinity of a time-independent massive spherically-symmetric body. In this section we recall some basic properties of the Schwarzschild solution.

The Schwarzschild metric is a static, spherically symmetric solution of the vacuum Einstein equations  $R_{ab} = 0$ . It is usually presented as

$$ds^2 = - \left(1 - \frac{2M}{r}\right) dt^2 + \left(1 - \frac{2M}{r}\right)^{-1} dr^2 + r^2(d\theta^2 + \sin^2\theta d\phi^2). \quad (1)$$

Here  $r$  is a radial coordinate such that the area of spheres at fixed  $r$  and  $t$  is  $4\pi r^2$ ; these spheres can be obtained invariantly by applying rotational isometries to a given initial point in the manifold. Each of these spheres are isometric to the standard round spheres in Euclidean space, and  $(\theta, \phi)$  are the usual polar coordinates. The time coordinate is  $t$ , and the metric is explicitly time independent in these coordinates. The parameter  $M$  is the mass and in non-geometrical units, we would have the replacement  $M \rightarrow GM/c^2$ . This metric turns out to be an excellent approximation to, say, the gravitational field in our solar system with the sun

treated as a point mass and with  $\phi(r) = GM/c^2 r$  being its Newtonian gravitational potential. The quantity  $R_s := 2GM/c^2$  is known as the Schwarzschild radius, and for the sun  $R_s \approx 3$  km (which agrees with the Michell-Laplace idea mentioned at the very beginning of this chapter).

The metric as written above is regular and non-degenerate for  $2M < r < \infty$  and  $-\infty < t < \infty$ . The singularity at  $r = 2M$  is not a true physical singularity [65] and can be removed by the transformation  $(t, r) \rightarrow (v, r)$  where

$$dv = dt + \left(1 - \frac{2M}{r}\right) dr. \quad (2)$$

In these coordinates (the ingoing Eddington-Finkelstein coordinates) the metric becomes

$$ds^2 = -\left(1 - \frac{2M}{r}\right) dv^2 + 2dv dr + r^2 d\Omega^2, \quad (3)$$

where  $d\Omega^2 := d\theta^2 + \sin^2\theta d\phi^2$ . The metric is now regular for  $r > 0$  and  $-\infty < v < \infty$ . We could extend the solution further by going to double null coordinates, but this shall suffice for now.

Consider now the vector fields

$$\ell = \frac{\partial}{\partial v} + \frac{1}{2} \left(1 - \frac{2M}{r}\right) \frac{\partial}{\partial r}, \quad n = -\frac{\partial}{\partial r}. \quad (4)$$

It is easy to check that these (future directed) vector fields are both null, i.e.  $\ell \cdot \ell = n \cdot n = 0$ , and  $\ell \cdot n = -1$ . By convention, we take  $\ell$  to be outward pointing and  $n$  to be inward pointing; we have designated  $r \rightarrow \infty$  to be “outwards”.

Let us pause to recall the notions of *expansion* and *shear* of a vector field. For a timelike vector field  $\xi$ , the set of vectors orthogonal to  $\xi$  form a three-dimensional plane at each point. If  $A$  is an infinitesimal area element in this plane and  $\lambda$  the affine parameter along  $\xi$ , then the expansion of  $\xi$  is defined as

$$\Theta_{(\xi)} = \frac{1}{A} \frac{dA}{d\lambda}. \quad (5)$$

Since a null vector field is orthogonal to itself, it is easy to show that any vector field  $V$  satisfying  $V \cdot \xi = 0$  can be written as a linear combination  $V = \alpha\xi + \beta\mathbf{e}_{(1)} + \gamma\mathbf{e}_{(2)}$  where  $\mathbf{e}_{(1)}$  and  $\mathbf{e}_{(2)}$  are mutually orthogonal unit spacelike vectors orthogonal to  $\xi$ , and  $\alpha, \beta, \gamma$  are real numbers. The expansion of  $\xi$  is then defined as in Eq. (5) above except that the relevant area element  $A$  is in the two-dimensional plane spanned by  $\mathbf{e}_{(1)}$  and  $\mathbf{e}_{(2)}$ . An alternate expression for the expansion which is usually more useful is

$$\Theta_{(\xi)} = q^{ab} \nabla_a \xi_b \quad (6)$$

where  $q^{ab}$  is the (inverse of) the Riemannian metric in the  $(e_{(1)}, e_{(2)})$  plane. The trace of  $\nabla_a \xi_b$  after projection is the expansion. The symmetric trace-free part and the antisymmetric parts give the shear  $\sigma_{ab}$  and twist  $\omega_{ab}$  respectively:

$$\sigma_{ab} = (\nabla_{(a} \xi_{b)})^\top - \frac{1}{2} \Theta_{(\xi)} q_{ab}, \quad \omega_{ab} = (\nabla_{[a} \xi_{b]})^\top. \quad (7)$$

where the symbol  $(\dots)^\top$  indicates a projection in the  $(e_{(1)}, e_{(2)})$  plane. The operators  $\sigma_{ab}$  and  $\omega_{ab}$  are responsible for transforming vectors in the  $(e_{(1)}, e_{(2)})$  plane. Consider now a set of neighboring null geodesics generated by  $\xi^a$ . Let  $\zeta^a$  be a connecting vector, i.e. it is transverse to  $\xi^a$  and is Lie dragged along  $\xi^a$ :  $\mathcal{L}_\xi \zeta^a = [\xi, \zeta]^a = \xi^b \nabla_b \zeta^a - \zeta^b \nabla_b \xi^a = 0$ . We get the effect

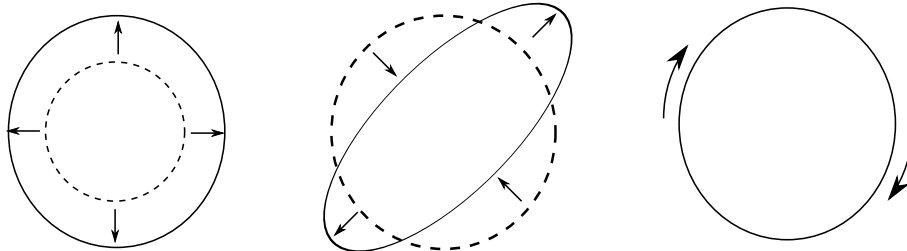


Figure 1: From left to right, an illustration of expansion, shear and twist respectively in the  $(e_{(1)}, e_{(2)})$  plane transverse to  $\xi^a$ , as illustrated by the effect on circles in this plane. The expansion  $\Theta_{(\xi)}$  is an isotropic expansion, the shear is an expansion and contraction in orthogonal directions with the area being preserved, and the twist is a rotation.

of the expansion, shear and twist as operators in the  $(e_{(1)}, e_{(2)})$  plane leading to the evolution of  $\zeta^a$  in time

$$\dot{\zeta}_b^\top := (\xi^a \nabla_a \zeta_b)^\top = \zeta^a (\nabla_a \zeta_b)^\top = \left( \sigma_{ab} + \omega_{ab} + \frac{1}{2} \Theta_{(\xi)} q_{ab} \right) \zeta^a. \quad (8)$$

The effect of expansion, shear and twist on  $\zeta^a$  is illustrated in Fig. 1. A particularly important result is the Raychaudhuri equation which gives the time derivative of the expansion for affinely parameterized null-geodesics:

$$\frac{d\Theta_{(\xi)}}{d\lambda} = -\frac{1}{2} \Theta_{(\xi)}^2 - \sigma_{ab} \sigma^{ab} + \omega_{ab} \omega^{ab} - T_{ab} \xi^a \xi^b. \quad (9)$$

This is a particular component of the Einstein field equations and a derivation and applications can be found in e.g. [39, 65]. We shall have occasion to use it at various points during the course of this chapter.

Returning to the vector fields  $\ell^a$  and  $n^a$  defined in Eq. (4), we see that they are manifestly orthogonal to the constant  $(v, r)$  spheres. Thus their expansions must involve area elements on these spheres and it is in fact easy to calculate their expansions:

$$\Theta_{(\ell)}(r) = \frac{r - 2M}{r^2}, \quad \Theta_{(n)}(r) = -\frac{2}{r}. \quad (10)$$

For spheres outside the black hole region, i.e. spheres with  $r > 2M$ , we see that  $\Theta_{(\ell)} > 0$  and  $\Theta_{(n)} < 0$ . This is how a round sphere in flat space behaves. However, for spheres in the black hole region, we get both expansions to be negative. Such spheres are known as trapped surfaces and play a fundamental role in black hole theory and, in particular, in the singularity theorems. The spheres on the  $r = 2M$  hyper-surface have  $\Theta_{(\ell)} = 0$ ,  $\Theta_{(n)} < 0$  and are called *marginally* trapped surfaces. Thus, we see that the  $r = 2M$  hyper-surface separates the region where the spherically symmetric trapped surfaces live and are a signature of a black hole spacetime. It is worth noting that the presence of trapped surfaces is not necessarily a signature of strong field gravity. The Riemann tensor (and thus the tidal force) is proportional to  $M/r^3$ . Thus at  $r = 2M$ , it is  $\propto 1/M^2$ , and large black holes have a correspondingly weaker curvature at their Schwarzschild radius. In this sense, trapped surfaces are a non-perturbative phenomena in general relativity. An observer falling into a sufficiently large black will not notice anything out of the ordinary.

The role of the  $r = 2M$  hyper-surface as the boundary of the region containing trapped surfaces (known as the trapped region) is typically not emphasized in standard textbooks on the subject. What is emphasized is instead the fact that starting from a point with  $r < 2M$ , there exist no timelike or null curves which can cross the  $r = 2M$  hyper-surface. This is easiest to visualize in a Penrose-Carter conformal diagram shown in Fig. 2. This is a convenient way of visualizing the  $r$ - $t$  part of the Schwarzschild metric. Just as we had extended the Schwarzschild metric in Eq. (1) across  $r = 2M$  by using ingoing null coordinates, we can extend the metric of Eq. (3) further by going to double null coordinates  $(u, v)$  where

$$du = dt - \left(1 - \frac{2M}{r}\right) dr, \quad dv = dt + \left(1 - \frac{2M}{r}\right) dr. \quad (11)$$

Fig. 2 is then obtained by performing a further re-scaling of coordinates and a conformal transformation which brings infinity to a finite distance. Details can be found in [65, 62] or in other standard textbooks on the subject. The original Schwarzschild metric is region I in this diagram while Eq. (3) corresponds to I and II. Regions III and IV are mirror images of I and II respectively. In this figure, null curves are straight lines at  $45^\circ$ ,  $i^0$  is spatial infinity,  $i^+$  is future timelike infinity and  $i^-$  is past timelike infinity. Future directed null curves in this figure end up either at the future singularity at  $r = 0$  (marked with a dashed line) or at future null-infinity labeled as  $\mathcal{S}^+$  ( $\mathcal{S}^-$  is past null-infinity). It is also worth pointing out that if region I is defined to be the “outside world” so that  $\ell^\alpha$  is the outward pointing null normal (this is merely a matter of convention), then  $\Theta_{(\ell)} < 0$  in regions II and III. However, region III has  $\Theta_{(n)} > 0$  so that only region II has both expansions negative. Similarly, only region IV has both expansions positive.

It is then clear that no point in region II can be connected with region I (or III) by a causal curve and thus justifies the term “black hole” for region II. The boundary of this region occurs at  $r = 2M$  and is called an event horizon. Note that the boundary of region IV also occurs at  $r = 2M$  but region IV is a time-reversed version of II; it has the property that no future directed causal curve can stay within it. Thus, region IV is called a white-hole. In the rest of this chapter, we shall only consider the portion of the  $r = 2M$  hyper-surface which bounds the black hole, i.e. region II. In a physical gravitational collapse situation, the white-hole (and region III) does not actually exist and is covered up by the matter fields which constitute the star; this will soon be seen explicitly when we study the Vaidya metric.

We thus have two different routes for describing a black hole: trapped surfaces versus event horizons (though one might suspect *a-priori* that the two might be intimately related). Trapped surfaces seem to be more local than event horizons. To know that a particular null geodesic will not leave a particular region of spacetime, one might need to know properties of the spacetime far away from the starting point of the geodesic. On the other hand, for trapped surfaces, in the Schwarzschild case we have just needed the computations of the expansions in Eq. (10) at a fixed value of  $(v, r)$ . However, one shouldn't forget that the computations of the expansions are not at just a single spacetime point, but are instead to be performed at all points over a sphere. This issue is irrelevant for spherically symmetric trapped surfaces in spherically symmetric spacetimes, but it is an important point that one cannot identify a trapped surface by examining only a part of it. For this reason, the trapped surface condition is said to be *quasi-local*. In any case, for Schwarzschild, the two descriptions of the black hole region agree: the  $r = 2M$  hyper-surface is both the event horizon and also the boundary of the region of spacetime which contains trapped surfaces.

Visualizing non-spherically symmetric trapped surfaces is harder, even in a spacetime as simple as Schwarzschild. As in many numerical investigations in general relativity, let us try to locate such surfaces on three-dimensional spatial hyper-surfaces. The equation  $\Theta_{(\ell)} = 0$  turns into a minimization problem, and to a second-order elliptic equation in three dimensional

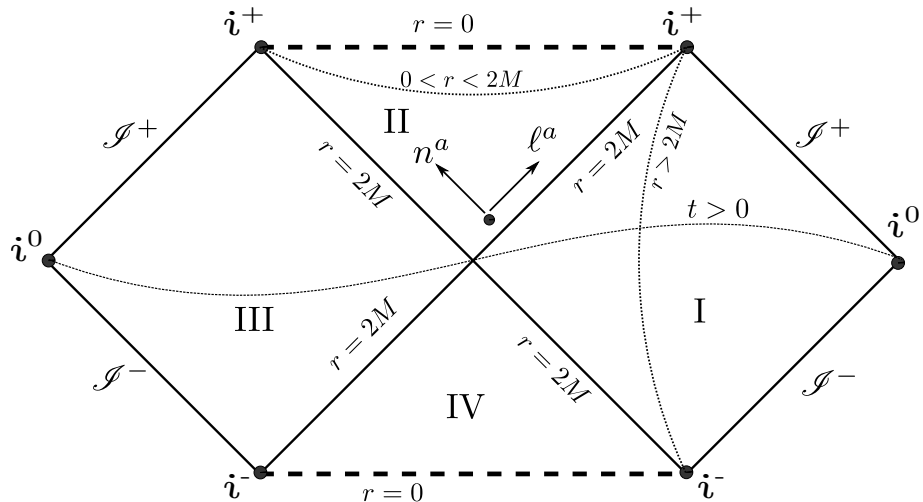


Figure 2: Penrose-Carter conformal diagram for the extended Schwarzschild spacetime. See text for details.

space (we shall have more to say on this matter later). The spatial hyper-surfaces depicted in Fig. 2 were all spherically symmetric, and thus a single curve in the Penrose diagram suffices for them. However, if we wish to depict non-spherically symmetric hyper-surfaces, we will need a collection of such curves, say one for each value of  $(\theta, \phi)$ . An example is shown in Fig. 3. In this example, the spatial hyper-surface starts from  $i^+$  on region III (but this detail is not important for our purposes and we could as well have started from  $i^0$  on the left edge of region III). What is important is that the spatial hyper-surfaces, or alternatively all the curves shown in Fig. 3 intersect the event horizon. As we shall see later, due to the somewhat non-intuitive properties of such null surfaces, the intersection of such a spatial hyper-surface with the  $r = 2M$  hyper-surface is still a marginally trapped surface though now a non-symmetric one. More specifically, it turns out that  $\ell_a$  is covariantly constant on the  $r = 2M$  surface so that  $\nabla_a \ell_b$ , projected onto the  $r = 2M$  surface, vanishes identically (see the discussion around Eq. (56) and in Sec. 4.4). This means that all closed cross-sections of the  $r = 2M$  surface are marginally trapped.

There would of course generally be non-spherically symmetric trapped surfaces on these spatial hyper-surfaces lying inside the marginally trapped one. Each spherically symmetric trapped and marginally trapped surface can be found by such a procedure. This construction clearly shows that there are many more non-symmetric trapped surfaces than symmetric ones; each spherically symmetric hyper-surface can be deformed in an infinite number of ways and still contain trapped and marginally trapped surfaces.

We note finally that it is possible to come up with examples where part of the spatial hyper-surface extends arbitrarily close to the future singularity, but part of it is still outside the black hole region so that its intersection with the event horizon is not a complete sphere. There would then exist no marginally trapped surfaces on such a spatial hyper-surface [66].

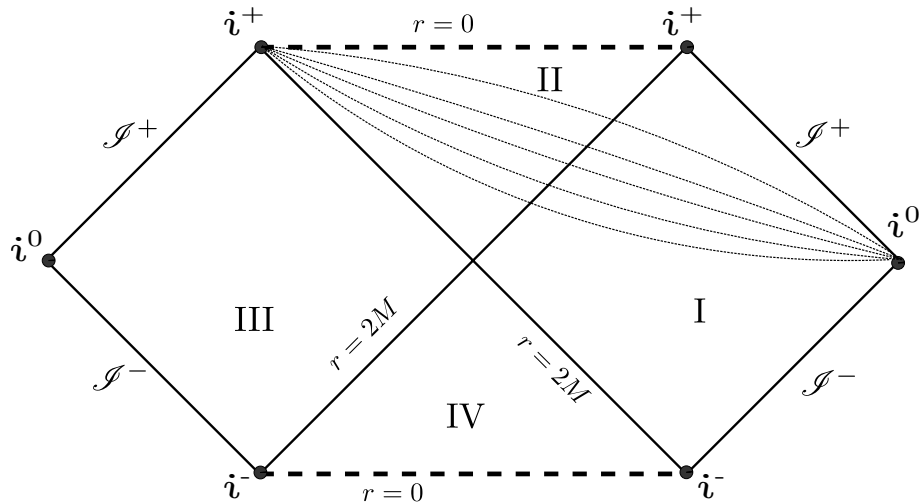


Figure 3: A non-spherically symmetric spatial hyper-surface in the Schwarzschild spacetime depicted as a set of curves.

## 2.2 The Vaidya spacetime

As we have just seen, for a Schwarzschild black hole, all the natural definitions of the surface of a black hole agree. Thus, the  $r = 2M$  surface is both the boundary of the trapped region and also the event horizon. This has led to a widespread belief that the notion of a black hole and its surface is unambiguous. Matters are however not so simple in dynamical situations. Let us now look at what is perhaps the simplest example of a dynamical black hole, namely the spherically symmetric Vaidya spacetime [64].

The Vaidya solution is obtained by starting with the Schwarzschild metric in ingoing Eddington-Finkelstein coordinates of Eq. (3), and replacing the constant  $M$  by a non-decreasing function  $M(v)$ :

$$ds^2 = - \left( 1 - \frac{2M(v)}{r} \right) dv^2 + 2dv dr + r^2 d\Omega^2. \quad (12)$$

The stress energy tensor for this metric is

$$T_{ab} = \frac{\dot{M}(v)}{4\pi r^2} \nabla_a v \nabla_b v, \quad \text{where} \quad \dot{M}(v) := \frac{dM(v)}{dv}. \quad (13)$$

This represents the collapse of null-dust to form a black hole and if  $\dot{M}(v) \geq 0$  then  $T_{ab}$  satisfies the dominant energy condition. If we choose a mass-function which is non-zero only for  $v > v_0$  and constant after  $v = v_1$ , then we will have (portions of) Minkowski and Schwarzschild spacetimes for  $v < v_0$  and  $v > v_1$  respectively. The Penrose-Carter diagram for this spacetime is shown in Fig. 4. A suitable set of null normals orthogonal to the constant  $(r, v)$  spheres are

$$\ell = \frac{\partial}{\partial v} + \frac{1}{2} \left( 1 - \frac{2M(v)}{r} \right) \frac{\partial}{\partial r}, \quad n = -\frac{\partial}{\partial r}, \quad (14)$$

and their expansions are respectively found to be

$$\Theta_{(\ell)}(v, r) = \frac{r - 2M(v)}{r^2}, \quad \Theta_{(n)}(v, r) = -\frac{2}{r}. \quad (15)$$



Thus, in this case, there are no spherically symmetric trapped surfaces outside the  $r = 2M(v)$  surfaces and as in Schwarzschild, the spheres with  $r = 2M(v)$  and fixed  $v$  are marginally trapped surfaces.

The event horizon is also not difficult to locate. Consider the outgoing null geodesics generated by the vector field  $\ell$  above. Some of these geodesics will reach infinity while others will terminate at the singularity. The event horizon is the boundary between the two cases. If we assume that the mass function reaches a finite final steady state value  $M_\infty$ , then the final black hole is a portion of Schwarzschild, and thus the condition  $r = 2M_\infty$  defines the final state of the event horizon. Thus, we want to find the outgoing null geodesic generated by  $\ell^a$  defined in Eq. (14) for which  $r \rightarrow 2M_\infty$  when  $v \rightarrow \infty$ . Subject to this final state boundary condition, we need to solve

$$\frac{dr}{dv} = \frac{1}{2} \left( 1 - \frac{2M(v)}{r} \right). \quad (16)$$

This is fairly easy to solve numerically for a generic mass function.

Let us now note a few properties of this event horizon. A typical case is shown in Fig. 4. First note that the event horizon extends to the flat region. A mortal observer in the flat region who has no way of knowing that the gravitational collapse will occur at some time in the future, might actually be living near an event horizon. The existence of the event horizon has really no consequences for any physical experiment or observations that the observer can conduct locally, and contrary to popular belief, the observer can cross the event horizon without feeling anything out of the ordinary. Furthermore, even an observer in the intermediate region  $v_0 < v < v_1$ , who can witness gravitational collapse occurring cannot know the true location of the event horizon. To illustrate this, consider Fig. 5. Here the mass function is non-zero for  $v < v_0$  as before, however, there are two phases. The mass function first reaches a constant value at  $v_1$  but restarts again at a later time  $v_2$ . The observer with  $v < v_2$  cannot know the value of  $M_\infty$  and can thus never know the true location of the event horizon.

### 2.2.1 Examples of non-symmetric trapped surfaces

In contrast to the event horizon, the  $r = 2M(v)$  surface seems to have the right properties. It bounds the region which has spherically symmetric trapped surfaces, it doesn't extend into the flat region, it grows only when  $\dot{M} > 0$ , it can be located quasi-locally, i.e. by checking the conditions for a trapped surface on a sphere, and it doesn't care about what happens to  $M(v)$  at late times. However, non-spherically symmetric trapped surfaces are not so well behaved. While there are no marginally trapped surfaces which lie completely within the flat region, we shall see that portions of them can extend into the flat region.

One can try to find marginally trapped surfaces numerically. The standard procedure is to start with a particular spatial hyper-surface  $\Sigma$ , and to find a surface  $S$  in  $\Sigma$  for which  $\Theta_{(\ell)} = 0$ . Let  $h_{ab}$  be the Riemannian metric on  $\Sigma$  induced by  $g_{ab}$ . If the unit normal on  $\Sigma$  is  $\hat{t}^a$ , the unit spacelike normal to  $S$  on  $\Sigma$  is  $\hat{r}^a$  with  $\ell^a = (\hat{t}^a + \hat{r}^a)/\sqrt{2}$  (see Fig. 6). With this choice, noting that the metric on  $S$  is  $q_{ab} = h_{ab} - \hat{r}_a \hat{r}_b = g_{ab} + \hat{t}_a \hat{t}_b - \hat{r}_a \hat{r}_b$ , the condition  $\Theta_{(\ell)} = 0$  can be written as

$$\sqrt{2}\Theta_{(\ell)} = \sqrt{2}q^{ab}\nabla_a \ell_b = D_a \hat{r}^a + K_{ab} \hat{r}^a \hat{r}^b - K = 0. \quad (17)$$

Here  $K_{ab} = h_a^c h_b^d \nabla_c \hat{t}_d$  is the extrinsic curvature,  $K$  is its trace, and  $D$  is the derivative operator on  $\Sigma$  (we shall explain these concepts in more detail later in Sec. 3.2). Taking coordinates  $(r, \theta, \phi)$  on  $S$  and assuming that the surface is given by an equation  $r = f(\theta, \phi)$ , the above equation becomes a non-linear second-order partial differential equation for  $f$  which can be solved numerically. Typical methods assume that the surface is *star-shaped*, i.e. every ray from the origin  $r = 0$  intersects the surface exactly once; for a more complete description of

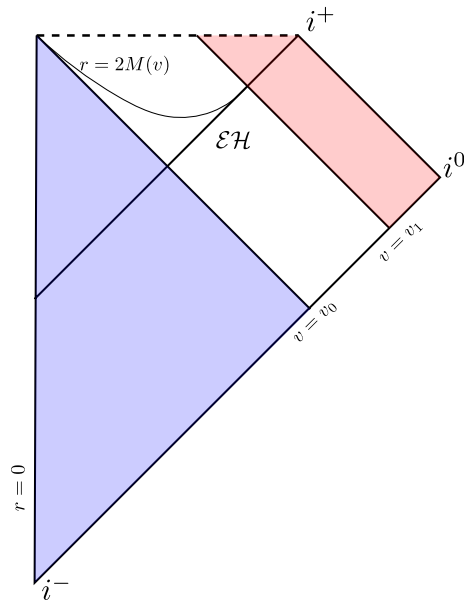


Figure 4: Penrose-Carter conformal diagram for the Vaidya spacetime. The region shaded in blue is flat and the region in red is isomorphic to a portion of Schwarzschild. The event horizon is labeled  $\mathcal{EH}$  and is seen to be distinct from the  $r = 2M(v)$  surface. The two agree only in the final Schwarzschild portion.

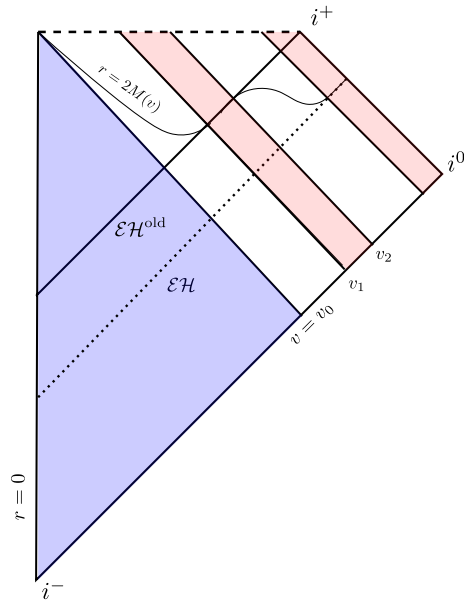


Figure 5: Another Penrose-Carter conformal diagram for the Vaidya spacetime. The region shaded in blue is again the flat region. The mass function here has two phases where it is increasing. An observer with  $v < v_2$  could in principle locate the solid line marked  $\mathcal{E}\mathcal{H}^{\text{old}}$  but will not know that the mass function will increase again and that the true event horizon is in fact given by the surface (indicated by a dotted line in this figure) marked  $\mathcal{E}\mathcal{H}$ .

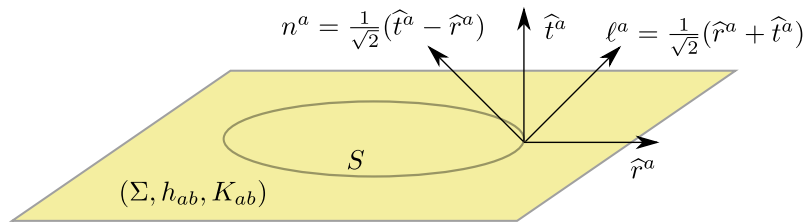


Figure 6: A closed marginally outer trapped surface on a spatial Cauchy surface  $\Sigma$  with intrinsic metric  $h_{ab}$  and extrinsic curvature  $K_{ab}$ . The unit timelike normal to  $\Sigma$  is  $\hat{t}^a$  and the outward unit spatial normal to  $S$  is  $\hat{r}^a$ . A particular choice of the out- and in-going null normals are  $\frac{1}{\sqrt{2}}(\hat{t}^a \pm \hat{r}^a)$ .

this and other methods, we refer to [63]. We then choose a particular mass function and a  $\Sigma$  defined through a particular non-axisymmetric time coordinate and attempt to locate surfaces with  $\Theta_{(\ell)} = 0$ . Let us review an illustrative result from a study reported in [60] (see also [55] for another such study) The particular mass function chosen corresponds to a short pulse of radiation:

$$M(v) = \begin{cases} 0 & \text{for } v \leq 0, \\ M_0 v^2 / (v^2 + W^2) & \text{for } v > 0. \end{cases} \quad (18)$$

The parameter  $M_0$  is the final mass and  $W$  determines the time-scale of the radiation pulse. We choose  $M_0 = 1$  and  $W = 0.1$ . The non-spherically symmetric time coordinate is taken to be

$$\bar{t} = v - r(1 + \alpha \cos \theta). \quad (19)$$

The constant  $\alpha$  determines the degree of asymmetry, and we choose  $\alpha = 10/11$ . As in Fig. 3, spatial hyper-surfaces of constant  $\bar{t}$  correspond to different sets of curves (one for each  $\theta$ ) in the Penrose-Carter diagram. Fig. 7 shows the marginal surface found on the  $\bar{t} = -0.3$  spatial hyper-surface. It shows the section in the  $x - z$  plane. The blue dotted line is the marginal surface, the green dashed line encloses the intersection of the flat region with the hyper-surface, and the solid red curve shows the intersection with the  $r = 2M(v)$  surface.  $\bar{t} = -0.3$  surface (which is not a marginal surface). Thus, we see that the marginal surface extends in the flat region, though in this example it is planar with  $\Theta_{(n)} = 0$  (so it is not, strictly speaking, a marginally trapped surface). The marginal surface is seen to be only partially inside the  $r = 2M(v)$  surface.

## 2.2.2 The trapped region

Having looked at particular examples of trapped surfaces in a Vaidya spacetime, let us consider the trapped region, i.e. the portion of the manifold which contains trapped surfaces. The trapped region for Vaidya spacetime can in fact be studied analytically. The starting point for this goes back to a conjecture by Eardley in 1998 [30]: *The outer boundary of the region containing outer trapped surfaces is the event horizon* (an outer trapped surface has  $\Theta_{(\ell)} < 0$  and no restriction on  $\Theta_{(n)}$ ). On the one hand, it is known that trapped surfaces cannot cross the event horizon. On the other hand, in dynamical situations like Vaidya, the event horizon is growing in area and its cross-sections are not marginally trapped. Thus, while the outer trapped surface might get arbitrarily close to the event horizon, the limiting process is not trivial. The Vaidya spacetime provides a relatively simple setting to study this phenomena.

Recent works in this direction have been [60, 21, 22, 23]). For any point  $p$  in the flat portion of the black hole region of the Vaidya spacetime, Ben-Dov showed [21] that there exists an

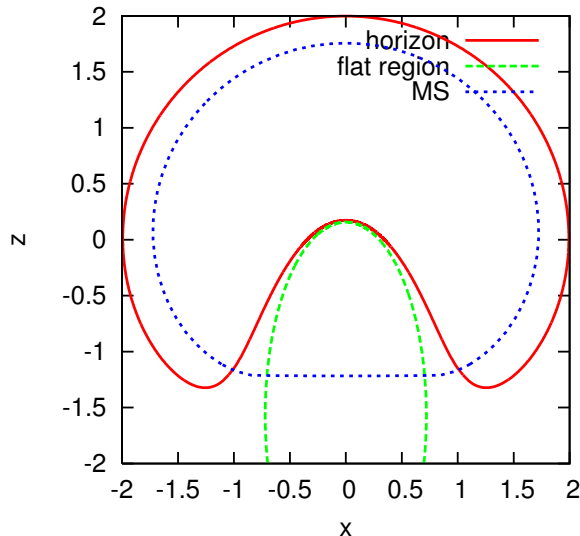


Figure 7: A non-symmetric closed surface in a particular Vaidya spacetime with  $\Theta_{(\ell)} = 0$  and  $\Theta_{(n)} \leq 0$ . The solid red curve is the intersection of the spatial hyper-surface with the  $r = 2M(v)$  surface, the green dotted line is the boundary of the flat region, and the blue dashed line is the marginal surface located on this spatial hyper-surface.

outer trapped surface  $S$  which contains  $p$ . This works even when  $p$  is arbitrarily close to the event horizon. In this case, most of the trapped surface actually lies inside the  $r = 2M(v)$  surface in the far future where  $v$  is large. There is a narrow “tendrill” which is almost null for a large portion, and yet stretches from the far future right down to the flat portion within the event horizon. This is precisely the kind of trapped surface whose existence was conjectured by Eardley in [30]. It is not clear that such highly non-symmetric trapped surfaces would be present in typical spatial hyper-surfaces used in numerical relativity simulations, or in fact, whether the standard numerical methods currently employed would be able to locate such a surface even if it were present.

It is also possible to locate the boundary of closed future trapped surfaces (i.e. surfaces with  $\Theta_{(\ell)} < 0$  and  $\Theta_{(n)} < 0$ ) in Vaidya spacetimes. The first result was obtained by Ben-Dov [21], but the complete solution to the problem was found by Bengtsson & Senovilla [22, 23]. Bengtsson & Senovilla have proved a number of results regarding the properties of trapped surfaces in spherically symmetric spacetimes, but here we shall only illustrate them by describing the past spacelike barrier for trapped surfaces in the Vaidya case. To this end, we need the following result (Theorem 4.1 of [23]): In a region  $\mathcal{R}$  of a spacetime, let  $\xi^a$  be a future pointing hyper-surface orthogonal vector field so that  $\xi_a = -F\nabla_a \bar{t}$  for some  $F > 0$  and some  $\bar{t}$  which increases to the future. If  $S$  is a future trapped surface which intersects  $\mathcal{R}$  (but is not necessarily contained within  $\mathcal{R}$ ), then  $S$  cannot contain a local minimum of  $\bar{t}$  at points with  $q^{ab}\mathcal{L}_{\xi}g_{ab} \geq 0$ .

In a region  $\mathcal{R}$  with a time coordinate such as  $\bar{t}$ , the significance of this result is that once a future trapped surface enters such a region with initially decreasing  $\bar{t}$  (i.e. if the surface is initially “bending downwards” in time), then  $\bar{t}$  must continue decreasing. If  $\mathcal{R}$  is bounded in the past by the event horizon, then clearly this result forces  $S$  to continue till it reaches the

event horizon. Since  $S$  cannot cross the event horizon (or even touch it), it becomes clear that the region  $\mathcal{R}$  cannot contain even portions of future trapped surfaces which are bending downwards in time. In Vaidya, an appropriate  $\xi$  is the so-called Kodama vector

$$\xi^a = \left( \frac{\partial}{\partial v} \right)^a \implies \xi_a = \nabla_a r - \left( 1 - \frac{2M(v)}{r} \right) \nabla_a v. \quad (20)$$

Since  $\xi_a \xi^a = -(1 - 2M(v)/r)$  it is clear that  $\xi^a$  is future directed to the past of the  $r = 2M(v)$  surface. Furthermore, it is easy to check that

$$\mathcal{L}_\xi g_{ab} = 2\dot{M}(v)\ell_a\ell_b. \quad (21)$$

Thus,  $q^{ab}\mathcal{L}_\xi g_{ab} \geq 0$  if  $\dot{M} \geq 0$ . The surfaces of constant  $\bar{t}$ , denoted by  $\Sigma^{\bar{t}}$  are spherically symmetric and defined by

$$\frac{dv}{dr} = \left( 1 - \frac{2M(v)}{r} \right)^{-1}. \quad (22)$$

If  $M(v)$  is constant for  $v > v_1$ , then there is a value of  $\bar{t} = \hat{t}$  such that  $\Sigma^{\bar{t}}$  coincides with the event horizon for  $v > v_1$ . Alternatively, if  $M(v)$  asymptotes to a constant value, then there is a value of  $\bar{t} = \hat{t}$  such that  $\Sigma^{\bar{t}}$  also asymptotes to the event horizon. In both these cases, let us denote these  $\Sigma^{\bar{t}}$  as  $\hat{\Sigma}$ . In the flat region,  $\Sigma^{\bar{t}}$  are horizontal lines in the Penrose diagrams. The behavior of  $\hat{\Sigma}$  depends sensitively on  $M(v)$ . In particular, it depends on the quantity  $\mu := \lim_{v \rightarrow 0} M(v)/v$ . When  $\mu > 1/8$ , it is shown in [23] that  $\hat{\Sigma}$  will enter the flat region, but in other cases it may not. These cases are depicted in Figs. 8a and 8b along with  $\Sigma^{\bar{t}}$  for some other values of  $\bar{t}$ . Any trapped surface which extends outside the  $r = 2M(v)$  surface must do so with increasing  $\bar{t}$  and it must never “bend” downwards in time. If it does not do so, then the above result shows that it must continue downwards till it hits the event horizon where it must cease to be smooth if the condition  $\Theta_{(\ell)} < 0$  condition is to be maintained (the event horizon is expanding and thus has positive expansion). It cannot terminate smoothly because this would imply the existence of a point on the trapped surface where  $\bar{t}$  is a local minimum.

A little thought then shows that  $\hat{\Sigma}$  must then be a past barrier which future trapped surfaces cannot cross. Furthermore, it is also clear that there cannot be any compact future trapped surface contained entirely in the region to the past of  $\hat{\Sigma}$ , and bounded between  $\hat{\Sigma}$  and the event horizon; if there were, again there would have to be a point on the trapped surface where  $\bar{t}$  is a local minimum. The boundary of the region containing trapped surfaces has thus been located. This boundary  $\hat{\Sigma}$  is of course spherically symmetric (as one can prove on general grounds). However, it is not foliated by marginally trapped surfaces. Thus, as with the limit of outer trapped surfaces to the event horizon, it is clear that the the limit of marginally trapped surfaces to this boundary cannot be smooth.  $\hat{\Sigma}$  is not a quasi-local object; it is as non-local as the horizon. Moreover, as far as we know, it does not have any features which might distinguish it as a black hole horizon.

### 2.2.3 Lessons from spherical symmetry

After this extensive discussion of the Schwarzschild and the Vaidya examples let us summarize the situation in spherical symmetry. We have seen the complications that can arise from having to consider non-spherically symmetric trapped surfaces in dynamical situations. In Schwarzschild there are no major surprises and any trapped surface can extend right up to the event horizon. This is not so in Vaidya; the obvious generalization of the  $r = 2M$  surface from Schwarzschild does not coincide with the event horizon. We need non-spherically symmetric trapped surfaces to “fill the gap” between the  $r = 2M(v)$  surface and the event horizon. It however turns out to be possible to study the trapped region in detail and to obtain a fairly

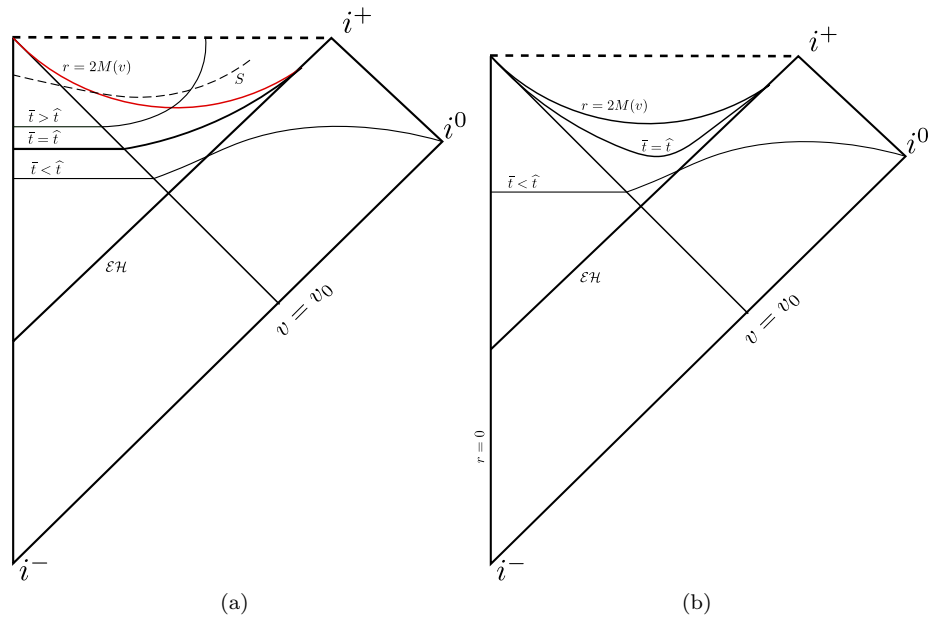


Figure 8: Surfaces of constant Kodama time for a Vaidya spacetime with  $\mu := \lim_{v \rightarrow 0} M(v)/v > 1/8$ . In this case  $\widehat{\Sigma}$  lies partially in the flat region. A future trapped surface which extends in the flat region is depicted as  $S$ . It required to enter the  $r > 2M(v)$  region with increasing  $\bar{t}$ . The right panel is similar to the left panel, but in this case  $\widehat{\Sigma}$  does not extend into the flat region. This happens for  $\mu \leq 8$ . A similar picture also works when  $M(v)$  asymptotes to a finite value for  $v \rightarrow \infty$ . This figure is essentially Fig. 15 of [23].

complete understanding of where trapped surfaces can (and cannot) occur. There turns out to be a difference between future- and outer-trapped surfaces (i.e. whether or not we consider the  $\Theta_{(n)} < 0$  condition). Outer trapped surfaces can extend all the way to the event horizon, but understanding how such surfaces limit to the event horizon is subtle; there is a separate past barrier for future trapped surfaces which is distinct from the event horizon.

What does this study tell us about non-spherically symmetric dynamical spacetimes? We note that the essential complication here, as noted by Eardley [30], is not that the black hole is non-spinning etc. Rather, the problem is to consider trapped surfaces which do not share the symmetry of the spacetime and to understand what happens to them as they are deformed towards the event horizon which will generally have positive expansion in dynamical situations. We might still expect outer trapped surfaces to extend to the event horizon in a similar fashion but there is, in general, probably no separate barrier for future trapped surfaces.

The next step in this chapter will be to study how marginally trapped surfaces evolve in time and under general deformations, and this leads to the subject of quasi-local horizons. However, before doing so, we shall first formalize many of the ideas introduced in this section with some general definitions and results.

### 3 General definitions and results: Trapped surfaces, stability and quasi-local horizons

#### 3.1 Event horizons

The surface of a black hole is traditionally defined in terms of an event horizon which is the boundary of the region from where massive or mass-less particles can reach the outside world. The formal definition is however more involved, with the main difficulty being in how the “outside world” is to be defined. It is worthwhile to briefly sketch the various technical ingredients that go into the precise formal definition, if only to highlight once again the truly global nature of event horizons; see e.g. [65, 39] for details.

This requires one to attach future and past null-infinity  $\mathcal{I}^\pm$  as boundaries to the physical spacetime and to consider the causal past of  $\mathcal{I}^+$ . This causal past is the region of spacetime  $\mathcal{R}$  from which causal signals can escape to infinity and represents the “outside-world”. The future boundary of  $\mathcal{R}$  is the event horizon. In Fig. 2, the region  $\mathcal{R}$  is the union of regions I, II and III, the black hole is of course region II and the portion of the  $r = 2M$  surface which divides region II from I and III is the event horizon. A little thought shows that in order for this notion to capture the physical idea we have in mind, it is necessary to ensure that  $\mathcal{I}^+$  is complete in an appropriate sense. For example, if we were to look at the causal past of just a portion of  $\mathcal{I}^+$  even for Minkowski space, we would erroneously conclude the presence of a black hole in Minkowski space [35]. Similarly for Schwarzschild, we could end up with the wrong location of the event horizon if we looked at only a portion of  $\mathcal{I}^+$  (see again Fig. 2).

Since we need to construct a complete  $\mathcal{I}^+$  and its global past in this definition, it is clear that the event horizon is a very global and teleological notion. There may in fact be an event horizon forming and growing in the room you are reading this article right now, because of possible events which might occur a billion years from now. An example is an observer in the flat region of the Vaidya spacetime in Fig. 4. This discussion also illustrates that formally, the notion of an event horizon cannot be used in a cosmological spacetime such as the one we inhabit, since it fails to be asymptotically flat.

In practice, the principle of calculating event horizons in numerical simulations is to start from an educated guess at late times, and to integrate a null geodesic or a null surface backwards in time [63, 28]. The basis for these methods is the fact that when we integrate forwards



in time, a small initial error will cause the null geodesic or surface to diverge exponentially from the true solution and end up either in the singularity or at infinity. This implies that by integrating backwards from even a reasonable guess at late times one will converge to the true solution exponentially.

### 3.2 Trapped surfaces

Let's begin with the standard definitions of the 1<sup>st</sup> and 2<sup>nd</sup> fundamental form of a smooth non-degenerate sub-manifold  $\widetilde{\mathcal{M}}$  embedded in a spacetime  $(\mathcal{M}, g_{ab})$ ; our discussion mostly follows [50]. The 1<sup>st</sup> fundamental form is just the induced metric  $h_{ab}$  on  $\widetilde{\mathcal{M}}$  so that for any vectors  $X^a$  and  $Y^b$  tangent to  $\widetilde{\mathcal{M}}$ :

$$h_{ab}X^aY^b := g_{ab}X^aY^b. \quad (23)$$

If  $h_{ab}$  is non-degenerate, we can decompose the tangent space  $T_p\mathcal{M}$  at any point  $p \in \widetilde{\mathcal{M}}$  as

$$T_p\mathcal{M} = T_p\widetilde{\mathcal{M}} \oplus T_p^\perp\widetilde{\mathcal{M}}, \quad T_p\widetilde{\mathcal{M}} \cap T_p^\perp\widetilde{\mathcal{M}} = \{0\}, \quad (24)$$

where  $T_p\widetilde{\mathcal{M}}$  is the tangent space to  $\widetilde{\mathcal{M}}$  and the subspace  $T_p^\perp\widetilde{\mathcal{M}}$  is normal to it. Thus, an arbitrary non-vanishing vector field  $\xi$  defined at points of  $\widetilde{\mathcal{M}}$  can be split uniquely into a tangential and normal part:

$$\xi = \xi^\top + \xi^\perp \quad \text{where} \quad \xi^\perp \cdot X = 0 \quad (25)$$

for any vector  $X$  tangent to  $\widetilde{\mathcal{M}}$ . Then, for any  $X, Y$  tangent to  $\widetilde{\mathcal{M}}$  we have

$$\nabla_X Y = (\nabla_X Y)^\top + (\nabla_X Y)^\perp. \quad (26)$$

The intrinsic covariant derivative on  $\widetilde{\mathcal{M}}$  is then defined as  $D_X Y := (\nabla_X Y)^\top$ . The 2<sup>nd</sup> fundamental tensor  $\Pi$  is an operator which takes two vectors tangent to  $\widetilde{\mathcal{M}}$  and produces a vector in the normal-subspace:  $T_p\widetilde{\mathcal{M}} \times T_p\widetilde{\mathcal{M}} \rightarrow T_p^\perp\widetilde{\mathcal{M}}$ :

$$\Pi(X, Y) := (\nabla_X Y)^\perp. \quad (27)$$

It is easy to show that  $D$  defined this way is a legitimate derivative operator, and that the 2<sup>nd</sup> fundamental form is symmetric:  $\Pi(X, Y) = \Pi(Y, X)$ . The symmetry of  $\Pi$  is especially easy:

$$\Pi(X, Y) - \Pi(Y, X) = (\nabla_X Y - \nabla_Y X)^\perp = [X, Y]^\perp = 0. \quad (28)$$

In the last step we have used the Frobenius theorem which says that for a smooth sub-manifold  $\widetilde{\mathcal{M}}$ , if  $X, Y$  are tangent to  $\widetilde{\mathcal{M}}$  then so is their commutator.

When  $\widetilde{\mathcal{M}}$  is a hyper-surface, i.e. when it has co-dimension 1, then  $N_p$  is 1-dimensional and spanned by the unit-normal  $N^a$ . Thus we can define the *extrinsic curvature*  $K_{ab}$  via

$$\Pi(X, Y)^c := -(K_{ab}X^aY^b)N^c. \quad (29)$$

The symmetry of  $\Pi$  implies that  $K_{ab} = K_{ba}$ . The most important case for us is however when the sub-manifold  $\mathcal{S}$  is 2-dimensional and spacelike; the 1<sup>st</sup> fundamental form, denoted by  $q_{ab}$  here, is a Riemannian metric on  $\mathcal{S}$ . We can again make the decomposition  $T_p\mathcal{M} = T_p\mathcal{S} \oplus T_p^\perp\mathcal{S}$ . The normal space  $T_p^\perp\mathcal{S}$  is a 1+1 dimensional Minkowski space. It will be convenient to choose two null vectors  $\ell$  and  $n$  to span  $T_p^\perp\mathcal{S}$ . We are of course free to re-scale  $\ell$  and  $n$  independently

by scalars, but we choose to use a normalization  $\ell \cdot n = -1$  which cuts down the re-scaling freedom to

$$\ell \rightarrow A\ell, \quad n \rightarrow A^{-1}n. \quad (30)$$

We will always choose  $(\ell, n)$  to be future directed and  $\ell$  and  $n$  as outward and inward pointing respectively. The *mean curvature* vector  $K^a$  is the trace of the 2<sup>nd</sup> fundamental form:

$$K^c := q^{ab}\Pi_{ab}{}^c = -\Theta_{(n)}\ell^c - \Theta_{(\ell)}n^c. \quad (31)$$

The coefficients appearing here turn out to be precisely the expansions  $\Theta_{(\ell, n)}$  discussed earlier. Under a re-scaling of the kind in Eq. (30),  $K^a$  remains invariant.

The different kinds of trapped surfaces correspond to properties of  $K^a$ . Two useful definitions are:

- *Future trapped surface* ( $\Theta_{(\ell)} < 0, \Theta_{(n)} < 0$ ):  $K^a$  is timelike and future-directed.
- *Marginally future trapped surface* ( $\Theta_{(\ell)} = 0, \Theta_{(n)} < 0$ ):  $K^a$  is null and future-directed.

Furthermore, we shall consider only *closed* surfaces; this is an important condition as it, among other things, excludes trivial planar surfaces in flat space.

It is also useful to remark on the physical significance of the condition  $\Theta_{(n)} < 0$ . This condition holds for round spheres in flat space and also, as we have seen, for round spheres in the trapped region of Schwarzschild (see Eq. (10)). However, this may not be true for non-spherically symmetric trapped surfaces even in Schwarzschild. Furthermore, there are explicit black hole solutions found by Geroch and Hartle [34] which represent black holes distorted by surrounding matter fields which do not satisfy  $\Theta_{(n)} < 0$  at all points on the horizon (but its average value over the horizon is still negative). In fact, for a number of key results that we shall mention below, it is not necessary to impose  $\Theta_{(n)} < 0$ . Surfaces with vanishing outward expansion  $\Theta_{(\ell)} = 0$ , with no restrictions on the sign of  $\Theta_{(n)}$  will be called *marginally outer trapped surfaces*, usually abbreviated to MOTS. A surface with  $\Theta_{(\ell)} < 0$  and no condition on  $\Theta_{(n)}$  will be said to be outer trapped. We have seen in the Vaidya example that there are differences in the location of trapped and outer trapped surfaces.

The collection of closed future-trapped surfaces form the trapped region of the spacetime. More precisely, the trapped region  $\mathcal{T}$  consists of spacetime points which lie on a closed future-trapped surface. The boundary  $\mathcal{B}$  of  $\mathcal{T}$  is the trapping boundary. It is also common to consider these concepts restricted to a spacelike surface  $\Sigma$ , typically a Cauchy surface in an initial value problem set-up. The trapped  $\mathcal{T}^\Sigma$  region on  $\Sigma$  is the set of points on  $\Sigma$  which lie on a closed future-trapped surface contained entirely on  $\Sigma$ . The boundary of  $\mathcal{T}^\Sigma$  is denoted  $\mathcal{B}^\Sigma$ , and each connected component of  $\mathcal{B}^\Sigma$  is called an *apparent horizon* if it is the outermost such boundary on  $\Sigma$ . Since  $\mathcal{B}^\Sigma$  excludes trapped surfaces not contained in  $\Sigma$ , it is clear that  $\mathcal{B}^\Sigma \subset \mathcal{B} \cap \Sigma$ . It is important to not confuse the trapped region  $\mathcal{T}$  or its boundary  $\mathcal{B}$  with the black hole region  $\mathcal{B}$  defined in Sec. 3.1 and the event horizon. It can be shown [42] that with some additional regularity conditions, each connected component of the apparent horizon  $\mathcal{B}^\Sigma$  is actually a closed marginally trapped surface. The same result was proved in [5] with the regularity assumptions removed. In practice, this fact is what is used to locate the apparent horizon in numerical simulations.

### 3.3 The stability of marginally trapped surfaces, trapping and dynamical horizons

Let us now go beyond individual trapped/marginally trapped surfaces and look at their time evolutions. Consider a region of spacetime foliated by smooth spacelike surfaces  $\Sigma^t$  depending on a real time parameter  $t$ . Start with initial data (the 1<sup>st</sup> and 2<sup>nd</sup> fundamental forms) at  $t = 0$

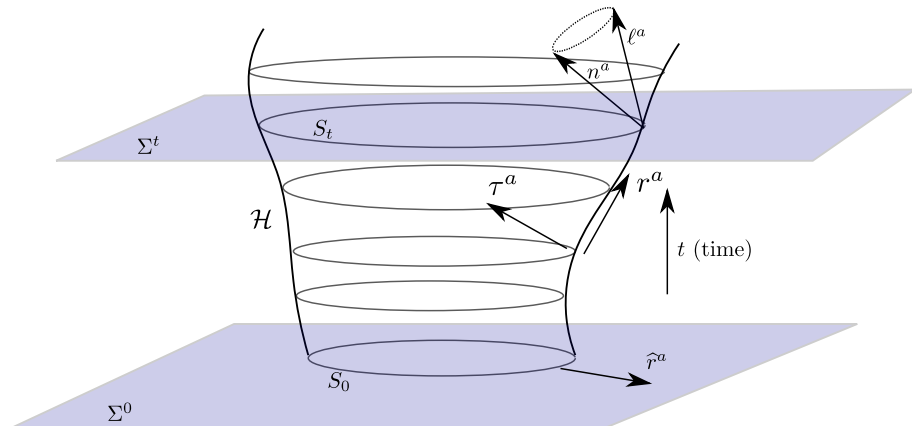


Figure 9: The evolution of a MOTS in time. Start at  $t = 0$  with a MOTS  $S_0$  on a spatial hypersurface  $\Sigma^0$ . Evolve the data on  $\Sigma^0$  using the Einstein equations. If the evolution of the MOTS is smooth in time, then  $S$  will evolve to a MOTS  $S_t$  on  $\Sigma^t$  at time  $t > 0$ . The collection of all the  $S_t$  will then form a smooth 3-surface  $\mathcal{H}$ . We shall see that  $\mathcal{H}$  will usually be spacelike so that the future null vectors  $\ell^a$  and  $n^a$  orthogonal to  $S_t$  (and the future null cone) will point “inwards” on  $\mathcal{H}$ . The vector  $\hat{r}^a$  is the unit outwards normal to  $S_t$  on  $\Sigma^t$ .

and evolve it using the Einstein and matter field equations. This way, we obtain a solution to the field equations locally in time near  $\Sigma^0$ . The first question we wish to address is: If  $\Sigma^0$  contains a MOTS  $S_0$ , does it persist under time evolution and does it evolve smoothly? If it does evolve smoothly, then the union of all the MOTS  $S^t$  will form a smooth 3-surface  $\mathcal{H}$  which we shall call a *marginally trapped tube* (MTT). A related question is then: How does  $\mathcal{H}$  depend on the foliation  $\Sigma^t$ ? If we start with the same  $\Sigma^0$  but choose the surfaces differently for  $t > 0$  (still requiring  $\Sigma^t$  to form a smooth foliation), then will we still end up with a smooth MTT  $\mathcal{H}'$ ? If it exists, is it different from  $\mathcal{H}$ ? In numerical simulations, it is found that the apparent horizon can evolve discontinuously. Can this be understood analytically?

It turns out that the answer to the above questions are intimately connected with the *stability* of  $S_0$  with respect to variations on  $\Sigma^0$ . To this end, we need to define the notion of the *geometric variation* of a 2-surface  $S$  which is embedded in a spacetime  $\mathcal{M}$  [54, 2, 4, 3]. Such a variation is a very general concept; it includes evolving in time, and an evolution following Einstein equations is a particular case. A smooth variation of a sub-manifold  $S$  is defined as a 1-parameter family of surfaces  $S_\lambda$  (where  $\lambda$  is a real parameter and takes values in some interval  $(-\epsilon, \epsilon)$ ) such that:  $S_0$  is identical to  $S$ , each  $S_\lambda$  is a smooth surface, and each point on  $S$  moves on a smooth curve as  $\lambda$  is varied. We can then define a vector field  $q^a$  as the tangent to these curves. This is depicted in Fig. 10. We could also perform the variation along null directions or spatial directions in a given spacetime and of course, the variations do not need to be uniform on  $S$  and different points on  $S$  can move at very different speeds depending on  $q^a$ .

If we have a relevant geometric quantity on  $S$ , we can compute it on each  $S_\epsilon$  and differentiate it with respect to  $\lambda$ , and the derivative is called the variation of that geometric quantity. If  $\mathcal{O}_\lambda$  is such a geometric quantity (e.g. the expansion  $\Theta_{(\ell)}$  on each  $S_\lambda$ ), then we shall define  $\delta_q \mathcal{O} := \partial_\lambda \mathcal{O}_\lambda|_{\lambda=0}$ . It is also important to keep in mind that for a function  $f$ , in general the variation is not linear:  $\delta_{fq} \mathcal{O} \neq f \delta_q \mathcal{O}$ .

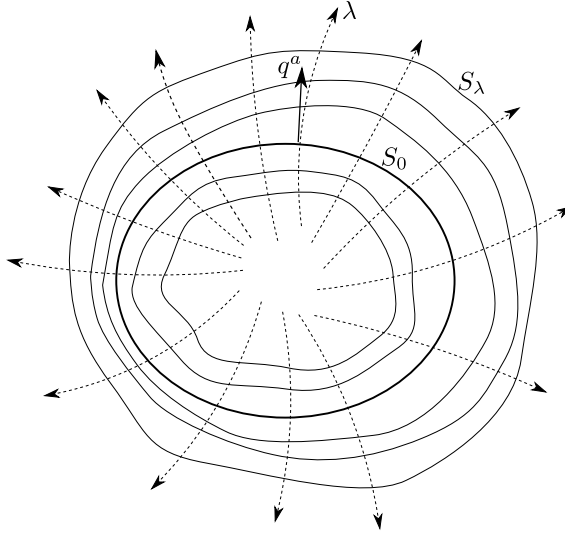


Figure 10: The variation of a surface  $S$  viewed as a set of surfaces  $S_\lambda$ . The initial surface is  $S_0$ . Each point on  $S$  moves along a smooth curve and  $q^a$  is the tangent to these curves.

For an MOTS defined on a spatial hyper-surface  $\Sigma$ , the relevant variation is along  $\hat{r}^a$ , the unit normal to  $S$ . The stability of  $S$  is meant to capture the idea that if  $S$  is deformed outwards, it becomes untrapped, and an inward deformation leads to  $\Theta_{(\ell)} < 0$ . No condition on  $\Theta_{(n)}$  is assumed. More precisely, the MOTS  $S$  is said to be *stably outermost* if there exists a function  $f \geq 0$  on  $S$  such that  $\delta_{f\hat{r}}\Theta_{(\ell)} \geq 0$ .  $S$  is *strictly stably outermost* if in addition  $\delta_{f\hat{r}}\Theta_{(\ell)} \neq 0$  somewhere on  $S$ .

With this background, we can state the following result [3, 4]: If  $S_0$  is a smooth MOTS on  $\Sigma^0$ , and  $S_0$  is strictly stably outermost on  $\Sigma^0$ , then  $S_0$  evolves smoothly into smooth MOTSs  $S_t$  on  $\Sigma^t$  at time  $t$  at least for sufficiently small (but non-zero)  $t$ . Furthermore, the union of the  $S_t$  forms a smooth 3-surface which we shall call  $\mathcal{H}$ . This holds at least as long as the  $S_t$  continue to remain strictly stable outermost. In addition, if  $G_{ab}\ell^a\ell^b > 0$  somewhere on  $S$  or if  $\ell^a$  has non-vanishing shear somewhere on  $S$ , then  $\mathcal{H}$  is spacelike. More generally, if the null energy condition holds then  $\mathcal{H}$  is either spacelike or null.

These results answer several of the questions raised at the beginning of this sub-section. If we were to start with the same  $\Sigma_0$  but choose different ones at later times, the MTT would still exist at least for some small time interval since the stability condition still holds at  $t = 0$ . However,  $\mathcal{H}'$  and  $\mathcal{H}$  would not necessarily coincide. The jumps that are observed in numerical simulations are because of the outermost condition: while an individual MTT can continue to evolve smoothly, a new MTT can appear further outwards. While not all MOTSs satisfy the stability condition, in all the cases that the author is aware of in numerical simulations, the MTTs continue to evolve smoothly. This suggests that the mathematical results could be strengthened.

Having seen that there is a physically interesting class of MOTSs which evolve smoothly in time, it is reasonable to impose additional conditions on an MTT to capture the fact that they are black hole horizons. The first is the notion of a *trapping horizon* defined by Hayward [41, 43] in 1994: A *future-outer-trapping horizon* (FOTH) is a smooth 3-dimensional manifold  $\mathcal{H}$  foliated by compact 2-manifolds  $S_t$  such that

1. The surfaces  $S$  are marginally trapped surfaces ( $\Theta_{(\ell)} = 0$ ,  $\Theta_{(n)} < 0$ ),
2. The directional derivative of  $\Theta_{(\ell)}$  along  $n^a$  vanishes:  $\mathcal{L}_n \Theta_{(\ell)} < 0$ .

Historically, this was the first systematic definition of a quasi-local horizon and it played a key role in spurring further developments. At the time, it was not known whether a MOTS would evolve smoothly in time and if trapped surfaces would limit smoothly to the boundary of the trapping region (as we have seen in the Vaidya example, they in fact do not and this possibility was recognized in [41]). Using this definition, Hayward showed that  $\mathcal{H}$  would be generically spacelike and is null if and only if the matter flux and the shear of  $\ell^a$  vanish identically (the result from [3, 4] quoted previously is stronger). Hayward also showed that it was possible to assign a surface gravity to the black hole, and to have versions of the laws of black hole mechanics applicable to  $\mathcal{H}$ . The second condition seems similar to the stability condition defined above, but in fact the two may not necessarily agree. A FOTH requires implicitly that  $\ell^a$  and  $n^a$  have been extended smoothly in a neighborhood of  $S$  and does not refer to the variation of  $S$ .

A *dynamical horizon* [14, 15] is defined similarly, but it is designed explicitly for the case when the horizon is spacelike: A smooth 3-dimensional manifold  $\mathcal{H}$  is said to be a *dynamical horizon* (DH) if it is foliated by compact 2-dimensional manifolds  $S_t$  such that

1. The surfaces  $S_t$  are marginally trapped ( $\Theta_{(\ell)} = 0$ ,  $\Theta_{(n)} < 0$ ).
2.  $\mathcal{H}$  is spacelike.

The first condition is the same as for a FOTH, but the second condition specifies *a-priori* the causal nature of  $\mathcal{H}$  without any additional conditions on fields transverse to  $\mathcal{H}$ . Even though the definitions of a FOTH and a DH are similar, neither implies the other. We shall return to dynamical and trapping horizons later in Sec. 5, but before that, we shall discuss the equilibrium case when the MTT is null in some detail.

## 4 The equilibrium case: Isolated horizons

Having discussed some general properties of trapped surfaces and their evolutions, we shall now consider a special case that is nevertheless of significant interest for various applications, namely when the black hole is in equilibrium with its surroundings and there is no matter or radiation falling into it. Since the work of the late 1990s and the subsequent years, our understanding of this special case has matured and we can now consider it to be well understood. All the well known globally stationary solutions in 4-dimensions, i.e the Kerr-Newman black holes, are included in this analysis. Also included are the dynamical cases when the black hole is itself in equilibrium but when the time dependent fields are relatively far away from the black hole. An example is a system of binary black holes when the separation of the black holes is much larger than either of the masses; to a very good approximation each black hole can be treated as being in equilibrium with its surroundings locally. In the same system, once the two black holes have coalesced, the final black hole will soon reach equilibrium after its ringdown phase. The assumption of global stationarity obviously does not hold in these cases. Each of these cases is well modeled by the framework of isolated horizons that we shall now describe. We shall start with a prototypical example namely, the structure of the horizon of a Kerr black hole. This shall be followed by a general definition and a summary of some key results. We shall conclude with two applications: the near horizon geometry and the mechanics of isolated horizons. It will be convenient to use the Newman-Penrose formalism in this discussion, and therefore we start with a short digression to discuss this formalism.

We note that strictly speaking, it is not essential to use this formalism for many of the results that we will discuss later. However, it does prove to be very useful in a number of

cases. For our purposes, we discuss it here because it makes calculations very explicit and is thus useful for pedagogically; there are no tensor indices and all geometric quantities are expressed in terms of scalar functions which have clear geometric and physical interpretations. Since we wish to start with the Kerr black hole as an example, this formalism is particularly useful for studying its properties explicitly.

## 4.1 The Newman-Penrose formalism

The Newman-Penrose formalism [52, 53] is a tetrad formalism where the tetrad elements are null vectors, which makes it especially well suited for studying null surfaces. See [56, 26, 62] for pedagogical treatments (note that these references take the spacetime metric to have a signature of  $(+ - - -)$  which is different from ours). Start with a null tetrad  $(\ell, n, m, \bar{m})$  where  $\ell$  and  $n$  are real null vectors,  $m$  is a complex null vector and  $\bar{m}$  its complex conjugate. The tetrad is such that  $\ell \cdot n = -1$ ,  $m \cdot \bar{m} = 1$ , with all other inner products vanishing. The spacetime metric is thus given by

$$g_{ab} = -\ell_a n_b - n_a \ell_b + m_a \bar{m}_b + \bar{m}_a m_b. \quad (32)$$

Directional derivatives along the basis vectors are denoted as

$$D := \ell^a \nabla_a, \quad \Delta := n^a \nabla_a, \quad \delta := m^a \nabla_a, \quad \bar{\delta} := \bar{m}^a \nabla_a. \quad (33)$$

We shall see that the Newman-Penrose formalism employs almost all the Greek symbols, and therefore often leads to conflicts in notation. An example is the symbol  $\Delta$  which is used for both the directional derivative along  $n^a$  and for the isolated horizon itself; we will have soon have other such examples. Hopefully the notation should be clear from the context.

The components of the connection are encoded in 12 complex scalars, the spin coefficients, defined via the directional derivatives of the tetrad vectors:

$$\left\{ \begin{array}{ll} D\ell & = (\epsilon + \bar{\epsilon})\ell - \bar{\kappa}m - \kappa\bar{m}, & (34a) \\ Dn & = -(\epsilon + \bar{\epsilon})n + \pi m + \bar{\pi}\bar{m}, & (34b) \\ Dm & = \bar{\pi}\ell - \kappa n + (\epsilon - \bar{\epsilon})m, & (34c) \\ \Delta\ell & = (\gamma + \bar{\gamma})\ell - \bar{\tau}m - \tau\bar{m}, & (34d) \\ \Delta n & = -(\gamma + \bar{\gamma})n + \nu m + \bar{\nu}\bar{m}, & (34e) \\ \Delta m & = \bar{\nu}\ell - \tau n + (\gamma - \bar{\gamma})m, & (34f) \\ \delta\ell & = (\bar{\alpha} + \beta)\ell - \bar{\rho}m - \sigma\bar{m}, & (34g) \\ \delta n & = -(\bar{\alpha} + \beta)n + \mu m + \bar{\lambda}\bar{m}, & (34h) \\ \delta m & = \bar{\lambda}\ell - \sigma n + (\beta - \bar{\alpha})m, & (34i) \\ \bar{\delta}m & = \bar{\mu}\ell - \rho n + (\alpha - \bar{\beta})m. & (34j) \end{array} \right.$$

While this kind of expansion may seem to some like a backwards step to the days before efficient tensor notation was developed, it is actually very convenient in cases where null vectors and null surfaces are involved. The use of complex functions is also efficient because it cuts down the number of quantities by half.

Many of the spin coefficients have a clear geometric meaning. First note that Eq. (34a) implies that  $\ell^a$  is geodesic if and only if  $\kappa = 0$ . Furthermore, it will be affinely parameterized if  $\epsilon + \bar{\epsilon} = 0$ . Similarly, from Eq. (34e), we see that  $n^a$  is geodesic if and only if  $\nu = 0$  and it is affinely parameterized if  $\gamma + \bar{\gamma} = 0$ . Important for us in particular are the coefficients  $\rho$  and  $\sigma$  which are related to the expansion, shear and twist defined earlier in Sec. 2.1. Let  $\ell^a$  be tangent to a null geodesic congruence, let it be affinely parameterized, and let  $\zeta^a$  be a connecting vector for the congruence (it is transverse to  $\ell^a$  and satisfies  $[\ell, \zeta] = 0$ ). As in Eq. 8,

we need to look at  $\nabla_a \ell_b$  projected in the  $(m, \bar{m})$  plane. Note that in this plane, the metric is  $q^{ab} = 2m^{(a} \bar{m}^{b)}$ , the antisymmetric area form is  ${}^2\epsilon = 2im^{[a} \bar{m}^{b]}$ , and the 2-dimensional space of symmetric trace-free  $2^{\text{nd}}$ -rank tensors is spanned by  $m^a m^b$  and  $\bar{m}^a \bar{m}^b$ . From the definitions above, it is easy to show that:

$$\Theta_{(\ell)} = q^{ab} \nabla_a \ell_b = m^a \bar{\delta} \ell_a + \bar{m}^a \delta \ell_a = -2\text{Re}\rho, \quad (35)$$

$$m^{[a} \bar{m}^{b]} \nabla_a \ell_b = \text{Im}\rho, \quad m^a m^b \nabla_a \ell_b = -\sigma. \quad (36)$$

Thus, we see that  $-2\text{Re}\rho$  is the expansion,  $\text{Im}\rho$  is related to the twist, and  $\sigma$  is the shear of  $\ell$ . Similarly, real and imaginary parts of  $\mu$  gives the expansion and twist of  $n^a$ , while  $\lambda$  yields its shear. It is also easy to verify that

$$[m, \bar{m}]^a = (\bar{\mu} - \mu)\ell^a + (\bar{\rho} - \rho)n^a + (\alpha - \bar{\beta})m^a + (\beta - \bar{\alpha})\bar{m}^a. \quad (37)$$

Thus, using the Frobenius theorem, we see that  $m$  and  $\bar{m}$  can be integrated to yield a smooth surface if  $\ell^a$  and  $n^a$  are twist free. Furthermore, since the projection of  $\delta m$  is determined by  $\beta - \bar{\alpha}$ , it is clear that this determines the connection, and thus the curvature of this surface.

Since the null tetrad is typically not a coordinate basis, the above definitions of the spin coefficients lead to non-trivial commutation relations:

$$\begin{cases} (\Delta D - D\Delta)f &= (\epsilon + \bar{\epsilon})\Delta f + (\gamma + \bar{\gamma})Df - (\bar{\tau} + \pi)\delta f - (\tau + \bar{\pi})\bar{\delta}f, & (38a) \\ (\delta D - D\delta)f &= (\bar{\alpha} + \beta - \bar{\pi})Df + \kappa\Delta f - (\bar{\rho} + \epsilon - \bar{\epsilon})\delta f - \sigma\bar{\delta}f, & (38b) \\ (\delta\Delta - \Delta\delta)f &= -\bar{\nu}Df + (\tau - \bar{\alpha} - \beta)\Delta f + (\mu - \gamma + \bar{\gamma})\delta f + \bar{\lambda}\bar{\delta}f, & (38c) \\ (\bar{\delta}\delta - \delta\bar{\delta})f &= (\bar{\mu} - \mu)Df + (\bar{\rho} - \rho)\Delta f + (\alpha - \bar{\beta})\delta f - (\bar{\alpha} - \beta)\bar{\delta}f. & (38d) \end{cases}$$

The Weyl tensor  $C_{abcd}$  breaks down into 5 complex scalars

$$\begin{cases} \Psi_0 = C_{abcd}\ell^a m^b \ell^c m^d, & \Psi_1 = C_{abcd}\ell^a m^b \ell^c n^d, & \Psi_2 = C_{abcd}\ell^a m^b \bar{m}^c n^d, & (39a) \\ \Psi_3 = C_{abcd}\ell^a n^b \bar{m}^c n^d, & \Psi_4 = C_{abcd}\bar{m}^a n^b \bar{m}^c n^d. & & (39b) \end{cases}$$

Similarly, the Ricci tensor is decomposed into 4 real and 3 complex scalars  $\Phi_{ij}$ :

$$\begin{cases} \Phi_{00} = \frac{1}{2}R_{ab}\ell^a \ell^b, & \Phi_{11} = \frac{1}{4}R_{ab}(\ell^a n^b + m^a \bar{m}^b), & \Phi_{22} = \frac{1}{2}R_{ab}n^a n^b, & \Lambda = \frac{R}{24}, & (40a) \\ \Phi_{01} = \frac{1}{2}R_{ab}\ell^a m^b, & \Phi_{02} = \frac{1}{2}R_{ab}\ell^a \bar{m}^b, & \Phi_{12} = \frac{1}{2}R_{ab}m^a n^b, & \bar{\Phi}_{ij} = \Phi_{ji}. & (40b) \end{cases}$$

We are allowed to make transformations of the null-tetrad while preserving their inner products, thereby leading to a representation of the proper Lorentz group. The allowed transformations are parameterized by two real parameters  $(A, \psi)$  and two complex numbers  $(a, b)$  (a total of six real parameters in all, as expected)

(i) Boosts:  $\ell \rightarrow A\ell, \quad n \rightarrow A^{-1}n, \quad m \rightarrow m$

(ii) Spin rotations in the  $m - \bar{m}$  plane:  $m \rightarrow e^{i\psi}m, \quad \ell \rightarrow \ell, \quad n \rightarrow n$

(iii) Null rotations around  $\ell$ :  $\ell \rightarrow \ell, \quad m \rightarrow m + a\ell, \quad n \rightarrow n + \bar{a}m + a\bar{m} + |a|^2\ell$

(iv) Null rotations around  $n$ :  $n \rightarrow n, \quad m \rightarrow m + b\ell, \quad \ell \rightarrow \ell + \bar{b}m + b\bar{m} + |b|^2n$

The transformations of the spin coefficients and curvature components under these transformations are not difficult to work out. Again, we refer to [56, 26, 62] for a more complete discussion.

The relation between the spin coefficients and the curvature components lead to the so called Newman-Penrose field equations which are a set of 16 complex first order differential equations. The Bianchi identities,  $\nabla_{[a}R_{bc]de} = 0$ , are written explicitly as 8 complex equations involving both the Weyl and Ricci tensor components, and 3 real equations involving only Ricci tensor components. See [56, 26, 62] for the full set of field equations and Bianchi identities.

## 4.2 The Kerr spacetime in the Newman-Penrose formalism

As the prototypical example for an isolated horizon, we now describe the structure of the Kerr black hole horizon. This will also illustrate the utility of the Newman-Penrose formalism when dealing with null surfaces. A detailed study of the various intricate properties of the Kerr spacetime can be found in [26]. Here we shall be brief and focus on the essential properties of the horizon.

The Kerr metric with mass  $M$  and spin  $a$  is usually presented in textbooks as (this is however not the form that Kerr originally derived it)

$$ds^2 = - \left(1 - \frac{2Mr}{\rho^2}\right) dt^2 + \frac{\rho^2}{\Delta} dr^2 - \frac{4aMr \sin^2 \theta}{\rho^2} dt d\phi + \rho^2 d\theta^2 + \frac{\Sigma^2 \sin^2 \theta}{\rho^2} d\phi^2 \quad (41)$$

where

$$\rho^2 = r^2 + a^2 \cos^2 \theta, \quad \Delta = r^2 - 2Mr + a^2, \quad \Sigma^2 = (r^2 + a^2)\rho^2 + 2a^2 Mr \sin^2 \theta. \quad (42)$$

This metric has two Killing vectors: a timelike one  $\xi^a = (\partial_v)^a$ , and a spacelike rotational one  $\varphi^a = (\partial_\phi)^a$ . Based on the behavior of the metric at large distances, one can assign a mass  $M_\infty = M$  and angular momentum  $J_\infty = aM$  to the spacetime. There are multiple ways to justify this. Because of the existence of the two Killing vectors, the clearest definition is through the so-called Komar integrals [48] based on the two Killing vectors (see also [65]). Moreover, again based on the behavior of the gravitational field at infinity, one can assign two sets of higher multipole moments  $M_k$  and  $J_k$  [33, 38, 18] which turn out to be fully determined by  $M$  and  $a$ :  $M_k + iJ_k = M(ia)^k$ ,  $k = 2, 3, \dots$

As in the original Schwarzschild metric, there are coordinate singularities when  $\Delta = 0$ . This happens when

$$r = r_\pm = M \pm \sqrt{M^2 - a^2}. \quad (43)$$

These can be removed by a coordinate transformation  $(t, r, \theta, \phi) \rightarrow (v, r, \theta, \varphi)$ :

$$dv = dt + \frac{r^2 + a^2}{\Delta} dr, \quad d\varphi = d\phi - \frac{a}{\Delta} dr. \quad (44)$$

This yields the metric in  $(v, r, \theta, \varphi)$  candidate

$$ds^2 = - \left(1 - \frac{2Mr}{\rho^2}\right) dv^2 + 2dv dr - 2a \sin^2 \theta dr d\varphi - \frac{4aMr \sin^2 \theta}{\rho^2} dv d\varphi + \rho^2 d\theta^2 + \frac{\Sigma^2 \sin^2 \theta}{\rho^2} d\varphi^2. \quad (45)$$

The horizon is the 3-dimensional surface  $r = r_+$  which we shall denote  $\Delta$ . The intrinsic metric  $q_{ab}$  on  $\Delta$  in  $(v, \theta, \varphi)$  coordinates is obtained by setting  $r = r_+$  and dropping the  $dr$  terms in this metric. Rearranging terms we get

$$q_{ab} = \frac{a^2 \sin^2 \theta}{\rho_+^2} (\nabla_a v - \Omega^{-1} d\varphi) (\nabla_b v - \Omega^{-1} d\varphi) + \rho_+^2 \nabla_a \theta \nabla_b \theta, \quad (46)$$



where  $\rho_+^2 := r_+^2 + a^2 \cos^2 \theta$  and  $\Omega = a/2Mr_+ = a/(r_+^2 + a^2)$ . It is easy to verify that this metric has signature  $(0 + +)$  with the degenerate direction being

$$\ell^a \nabla_a = \frac{\partial}{\partial v} + \Omega \frac{\partial}{\partial \varphi}. \quad (47)$$

Thus, the null normal to  $\Delta$  acquires an angular velocity term in the presence of spin.

The cross sections of this manifold, i.e. the surfaces of constant  $v$ , are spheres with a Riemannian metric  $\tilde{q}_{ab}$ . The area of such a sphere is time independent:  $a_\Delta = 4\pi(r_+^2 + a^2)$ . It is easy to verify that if we choose a different coordinate  $v'$  with the cross-sections still being complete spacelike spheres, the area of each cross section is still  $a_\Delta$ .

A suitable choice of the ingoing and outgoing future directed null vectors are

$$n^a \nabla_a = - \left( \frac{r^2 + a^2}{\rho^2} \right) \frac{\partial}{\partial r}, \quad \ell^a \nabla_a = \frac{\partial}{\partial v} + \frac{a}{r^2 + a^2} \frac{\partial}{\partial \varphi} + \frac{\Delta}{2(r^2 + a^2)} \frac{\partial}{\partial r}. \quad (48)$$

On  $\Delta$   $\ell^a$  agrees with the null direction given in Eq. (47). The other null vector  $n^a$  is clearly null because the metric does not have a  $dr^2$  term, and the scalar factor in  $n^a$  is chosen to ensure  $\ell \cdot n = -1$ . The covariant versions are:

$$n_a = \frac{r^2 + a^2}{\rho^2} (-\nabla_a v + a \sin^2 \theta \nabla_a \varphi), \quad \ell_a = -\frac{\Delta}{2(r^2 + a^2)} \nabla_a v + \frac{\rho^2}{r^2 + a^2} \nabla_a r + \frac{\Delta a \sin^2 \theta}{2(r^2 + a^2)} \nabla_a \varphi. \quad (49)$$

A suitable choice for  $m^a$  is

$$\begin{aligned} m_a &= -\frac{a \sin \theta}{\sqrt{2\tilde{\rho}}} \nabla_a v + \frac{(r^2 + a^2) \sin \theta}{\sqrt{2\tilde{\rho}}} \nabla_a \varphi + \frac{i}{\sqrt{2}} \tilde{\rho} \nabla_a \theta, \\ m^a \nabla_a &= \frac{a \sin \theta}{\sqrt{2\tilde{\rho}}} \frac{\partial}{\partial v} + \frac{1}{\sqrt{2\tilde{\rho}} \sin \theta} \frac{\partial}{\partial \varphi} + \frac{i}{\sqrt{2\tilde{\rho}}} \frac{\partial}{\partial \theta}. \end{aligned} \quad (50)$$

Here we have defined  $\tilde{\rho} := r + ia \cos \theta$ , so that  $\rho^2 = |\tilde{\rho}|^2$ . It is unfortunate that the notation can be confusing. For example the  $\rho^2$  used in the Kerr metric is not to be confused with the spin coefficient  $\rho$ . This should hopefully not cause confusion because the spin coefficient  $\rho$  will vanish identically, and unless mentioned otherwise,  $\rho^2$  will refer to  $r^2 + a^2 \sin^2 \theta$ .

We can now compute the spin coefficients at  $\Delta$  and for the moment we shall restrict our attention to those spin coefficients which are intrinsic to  $\Delta$ , i.e. do not require any derivatives transverse to  $\Delta$ . These are:  $\epsilon, \kappa, \pi, \alpha, \beta, \rho, \sigma, \mu, \lambda$ . As is typical in tetrad formalisms, we do not need to compute any Christoffel symbols in order to compute any of the spin coefficients; the exterior derivative suffices. Using the definitions of Eq. (34) we can write the exterior derivatives of  $\ell_a, m_a, n_a$  in terms of the exterior products of the basis vectors. The spin coefficients are then combinations of contractions of the exterior derivatives with the basis vectors. As an example, the acceleration of  $\ell^a$  and its value at the Kerr horizon is

$$\epsilon + \bar{\epsilon} = \ell^b n^a \cdot 2\nabla_{[a} \ell_{b]} = \frac{r_+ - M}{2Mr_+} = \frac{\sqrt{M^2 - a^2}}{2M(M + \sqrt{M^2 - a^2})}. \quad (51)$$

The other spin coefficients at the horizon turn out to be:

$$\kappa = \sigma = \rho = \lambda = \nu = 0, \quad \pi = \alpha + \bar{\beta} = -\frac{\sqrt{2}ar \sin \theta}{\rho^2 \tilde{\rho}} \quad (52)$$

Some of these can be understood on general grounds. First, since  $\ell^a$  is tangent to a smooth surface, it must be hyper-surface orthogonal which means that we must have  $\text{Im}\rho = 0$ . Furthermore, if a null vector is hyper-surface orthogonal, it can be shown to be tangent to a

geodesic. This implies  $\kappa = 0$ . The important condition on physical grounds is that the expansion of  $\ell^a$  vanishes:  $\text{Re}\rho = 0$ . Thus, as we saw for a Schwarzschild black hole, the cross sections of  $\Delta$  are marginally outer trapped surfaces. Now let us turn to the Weyl tensor. It can be shown that the only non-zero component is

$$\Psi_2 = -\frac{M}{(r - ia \cos \theta)^3}. \quad (53)$$

Can we now extract from these results general properties of a null surface which should behave like a black hole horizon in equilibrium? Can we assign physical quantities such as surface gravity, mass, angular momentum and higher multipole moments? We shall answer these questions in the next sub-section. Regarding angular momentum, we note that the spin coefficient which vanishes for  $a = 0$  is  $\pi$ . In fact, from the values of the spin coefficient, we can check that for any  $X^a$  tangent to the horizon,  $X^a \nabla_a \ell^b = X^a \omega_a \ell^b$  where

$$\omega_a := -(\epsilon + \bar{\epsilon})n_a + \pi m_a + \bar{\pi} \bar{m}_a. \quad (54)$$

We shall see that the angular part of  $\omega_a$  yields the angular momentum of the horizon.

### 4.3 A primer on null-hyper-surfaces

The fundamental geometric objects in the theory of isolated horizons are null surfaces. Let us therefore start with a discussion of the geometry of null surfaces in a Lorentzian manifold. The horizon of a Kerr black hole is a special kind of null surface, namely an expansion and shear free null surface. Such null surfaces are rather special from a geometrical point of view as we shall now explain.

Consider a smooth sub-manifold  $\widetilde{\mathcal{M}}$  of a spacetime  $(\mathcal{M}, g_{ab})$ . As earlier in Sec. 3.2, we define the 1<sup>st</sup>-fundamental tensor of  $\widetilde{\mathcal{M}}$ , i.e. the induced metric  $h_{ab}$  as the restriction of  $g_{ab}$  to  $\widetilde{\mathcal{M}}$ :  $h_{ab}X^aY^b := g_{ab}X^aY^b$  for any two-arbitrary vector fields  $X^a$  and  $Y^b$  tangent to  $\widetilde{\mathcal{M}}$ . The sub-manifold  $\widetilde{\mathcal{M}}$  is said to be null when  $h_{ab}$  is degenerate. In the non-degenerate case, the ambient covariant derivative operator  $\nabla$  induces a natural derivative operator  $\mathcal{D}$  on  $\widetilde{\mathcal{M}}$ . Furthermore,  $\mathcal{D}$  is the unique derivative operator compatible with  $h_{ab}$ , i.e.  $\mathcal{D}_a h_{bc} = 0$ .

Can we repeat the steps described in Sec. (3.2) for defining the fundamental forms and intrinsic connection on a null surface? When  $\widetilde{\mathcal{M}}$  is a null hyper-surface, we shall call  $\ell^a$  a null normal if it is along the degenerate direction of  $h_{ab}$ , so that  $h_{ab}\ell^a = 0$ . We thus encounter a problem in the very first step, i.e. in the decomposition of Eq. (24). The null normal  $\ell^a$  is also tangent to  $\widetilde{\mathcal{M}}$  so that  $T_p\widetilde{\mathcal{M}} \cap T_p^\perp\widetilde{\mathcal{M}} \neq \{0\}$ . The other route to defining  $\mathcal{D}$ , namely finding the unique derivative operator compatible with  $h_{ab}$  doesn't work either because a degenerate metric does not uniquely determine a derivative operator. We can still define an intrinsic derivative operator  $\mathcal{D}$  if we pick a particular subspace of  $T_p\widetilde{\mathcal{M}}$  transverse to  $\widetilde{\mathcal{M}}$ . Following [19], we first pick a spacelike subspace  $\mathcal{S}_p$  of  $T_p\widetilde{\mathcal{M}}$ ; for the Kerr horizon, a natural choice would be vectors tangent to the spherical cross-sections of fixed  $v$ . There will be two 1-dimensional sub-spaces of null vectors orthogonal to  $\mathcal{S}_p$ . One of them is  $N_p\widetilde{\mathcal{M}}$ , the null direction of  $h_{ab}$  and the other will be transverse to  $\mathcal{M}$  which we shall call  $N'_p\widetilde{\mathcal{M}}$ , and we can decompose  $T_p\mathcal{M}$  as  $T_p\widetilde{\mathcal{M}} \oplus N_p\widetilde{\mathcal{M}} \oplus N'_p\widetilde{\mathcal{M}}$ . Associated to a particular null normal  $\ell^a$  we shall pick a vector  $n^a$  in the transverse direction by requiring that  $\ell \cdot n = -1$ . We can then decompose  $\xi$  as

$$\xi = \xi^\top + \xi^\perp \quad \text{where} \quad \begin{aligned} \xi^\top &:= \widetilde{\xi} + \alpha \ell \\ \xi^\perp &:= \beta n \end{aligned} \quad (55)$$

Here  $\alpha$  and  $\beta$  are scalars,  $\widetilde{\xi}$  is in  $\mathcal{S}_p$  at each  $p$ . We can then define the intrinsic derivative operator as before:  $\mathcal{D}_X Y = (\nabla_X Y)^\top$ . However,  $\mathcal{D}$  would depend on our choice of  $\mathcal{S}_p$  and

unlike in the non-degenerate case, there is in general no natural canonical choice. There is however one case when this is not an issue, namely when the 2<sup>nd</sup>-fundamental form vanishes,  $\nabla_X Y$  is always tangential to  $\widetilde{\mathcal{M}}$  and there is no need to decompose  $\nabla_X Y$ . This happens when:

$$\ell_a X^b \nabla_b Y^a = -X^a Y^b \nabla_a \ell_b = 0 \quad (56)$$

for any  $X^a, Y^a$  tangent to  $\widetilde{\mathcal{M}}$ . Thus,  $\ell_a$  is covariantly constant on the null surface.

An alternative way to state the same result (emphasized in e.g. [8]) is: if we start with a vector tangent to  $\Delta$  and parallel transport it using the spacetime derivative operator  $\nabla$  along a curve lying on  $\Delta$ , then the vector remains tangent to  $\Delta$ . Since parallel transport of  $Y^a$  along  $X^a$  is defined by  $X^a \nabla_a Y^b = 0$ , this alternative criteria is also equivalent to  $\ell_a X^b \nabla_b Y^a = 0$ . We shall see that Eq. (56) is satisfied for the various kinds of horizons that we shall now define.

#### 4.4 Non-expanding, weakly-isolated and isolated horizons

Having understood null-surfaces, we are now ready to define different kinds of isolated horizons with increasingly stronger conditions. We shall start with the minimum set of conditions, namely a marginally trapped tube which is null, and no condition on the ingoing expansion. A smooth 3-dimensional null surface  $\Delta$  is said to be a *non-expanding horizon* if:

- $\Delta$  has topology  $S^2 \times \mathbb{R}$ , and if  $\varpi : S^2 \times \mathbb{R} \rightarrow S^2$  is the natural projection, then  $\varpi^{-1}(x)$  for any  $x \in S^2$  are null curves on  $\Delta$ .
- The expansion  $\Theta_{(\ell)} := q^{ab} \nabla_a \ell_b$  of any null normal  $\ell^a$  of  $\Delta$  vanishes.
- The Einstein field equations hold at  $\Delta$ , and the matter stress-energy tensor  $T_{ab}$  is such that for any future directed null-normal  $\ell^a$ ,  $-T_b^a \ell^b$  is future causal.

We shall consider only null tetrads adapted to  $\Delta$  such that, at the horizon,  $\ell^a$  coincides with a null-normal to  $\Delta$ . We shall also consider a foliation of the horizon by spacelike spheres  $S_v$  with  $v$  a coordinate on the horizon which is also an affine parameter along  $\ell$ :  $\mathcal{L}_\ell v = 1$ ;  $S$  shall denote a generic spherical cross-section of  $\Delta$ . Null rotations about  $\ell^a$  correspond to changing the foliation.

This deceptively simple definition of a non-expanding horizon leads to a number of important results which we state here without proof, most of which are however well illustrated by the Kerr example discussed earlier.

1. Any null normal  $\ell^a$  is a symmetry of the intrinsic degenerate metric  $q_{ab}$  on  $\Delta$ :  $\mathcal{L}_\ell q_{ab} = 0$ .
2. The null normal of  $\Delta$  is only given to be expansion free. However, a non-expanding horizon is also shear free. To show this, we use the Raychaudhuri equation:

$$\mathcal{L}_\ell \Theta_\ell = \kappa_\ell \Theta_{(\ell)} - \frac{1}{2} \Theta_{(\ell)}^2 - |\sigma|^2 - R_{ab} \ell^a \ell^b. \quad (57)$$

Setting  $\Theta_{(\ell)} = 0$ , and observing that the energy condition implies  $R_{ab} \ell^a \ell^b \geq 0$ , we get that the sum of two non-negative quantities must vanish.

$$|\sigma|^2 + R_{ab} \ell^a \ell^b = 0. \quad (58)$$

This can only happen if  $\sigma = 0$  and  $R_{ab} \ell^a \ell^b = 0$  on the horizon. Thus, the full projection of  $\nabla_a \ell_b$  on  $\Delta$  vanishes, and as we saw in Sec. 4.3, this is just the condition required to ensure that the induced derivative operator on  $\Delta$  is well defined.

3. The Weyl tensor components  $\Psi_0$  and  $\Psi_1$  vanish on the horizon. This implies that  $\Psi_2$  is an invariant on  $\Delta$  as long as the null-tetrad is adapted to the horizon; it is automatically invariant under boosts and spin rotations (it has spin weight 0), and it is invariant under null rotations around  $\ell$  because  $\Psi_0$  and  $\Psi_1$  vanish. Similarly, the Maxwell field component  $\phi_0$  vanishes on the horizon, and  $\phi_1$  is invariant on  $\Delta$ . Both  $\Psi_2$  and  $\phi_1$  are also time independent on the horizon.
4. There exists a 1-form  $\omega_a$  such that, for any vector field  $X^a$  tangent to  $\Delta$ ,

$$X^a \nabla_a \ell^b = X^a \omega_a \ell^b. \quad (59)$$

The 1-form  $\omega_a$  plays a fundamental role in what follows. The pullback of  $\omega_a$  to the cross-sections  $S$  will be denoted  $\tilde{\omega}_a$ .

5. The surface gravity of  $\ell$  is

$$\tilde{\kappa}_{(\ell)} = \ell^a \omega_a. \quad (60)$$

We will say that  $\Delta$  is extremal if  $\tilde{\kappa}_{(\ell)} = 0$  and non-extremal otherwise. Here we shall always assume that  $\Delta$  is non-extremal. The curl and divergence of  $\omega$  carry important physical information. The curl is related to the imaginary part of the Weyl tensor on the horizon

$$d\omega = \text{Im}[\Psi_2]^2 \epsilon. \quad (61)$$

and its divergence specifies the foliation of  $\Delta$  by spheres [9].

6. By the geometry of  $\Delta$ , we shall mean the pair  $(q_{ab}, \mathcal{D}_a)$ . Clearly,  $q_{ab}$  yields a Riemannian metric  $\tilde{q}_{ab}$  on the cross-sections of  $\Delta$ . In turn,  $\mathcal{D}_a$  is determined by  $\omega_a$  and by the unique derivative operator  $\tilde{\mathcal{D}}_a$  compatible with  $\tilde{q}_{ab}$ .

We need to strengthen the conditions of a non-expanding horizon for various physical situations. The minimum extra condition required for black hole thermodynamics and to have a well defined action principle with  $\Delta$  as an inner boundary of a portion of spacetime, is formulated as a weakly isolated horizon [12]: A weakly isolated horizon  $(\Delta, [\ell])$  is a non-expanding horizon equipped with an equivalence class of null normals  $[\ell]$  related by constant positive rescalings and such that

$$\mathcal{L}_\ell \omega_a = 0. \quad (62)$$

If we rescale  $\ell \rightarrow f\ell$ ,  $\omega_a$  transforms as  $\omega_a \rightarrow \omega_a + \partial_a \ln f$ . It is thus invariant under constant rescalings and there is a unique  $\omega_a$  corresponding to the equivalence class  $[\ell]$ .

The zeroth law holds on weakly isolated horizons, i.e.  $\tilde{\kappa}_{(\ell)} = \ell^a \omega_a$  is constant on  $\Delta$ :

$$\mathcal{L}_\ell \omega_a = \ell^b 2\mathcal{D}_{[b} \omega_{a]} + \mathcal{D}_a(\ell^b \omega_b) = \mathcal{D}_a \tilde{\kappa}_{(\ell)}. \quad (63)$$

In the second step we have used Eq. (61) to conclude that  $\ell^b \times 2\mathcal{D}_{[b} \omega_{a]} = \text{Im}\ell^b [\Psi_2]^2 \epsilon_{ba} = 0$ . Note that under a re-scaling  $\ell^a \rightarrow f\ell^a$ ,  $\omega_a$  transforms as  $\omega_a \rightarrow \omega_a + D_a \ln f$  so that it is invariant under constant rescalings.

Any non-expanding horizon can be made into a weakly isolated horizon by suitably scaling the null generators. Thus, the restriction to weakly isolated horizons is not a genuine physical restriction. One could go ahead and impose further physical restrictions on the intrinsic horizon geometry by requiring that not only  $\omega_a$ , but the full connection  $\mathcal{D}_a$  on  $\Delta$  is preserved by  $\ell^a$ : An isolated horizon  $(\Delta, [\ell])$  is thus a non-expanding horizon equipped with an equivalence class of null-normals related by constant positive rescalings such that  $[\mathcal{L}_\ell, \mathcal{D}] = 0$  [9].

It can be shown that the gauge-invariant geometry of an axisymmetric isolated horizon can be fully specified by the area  $a_\Delta$  and two set of multipole moments  $M_n, J_n$  for  $n = 0, 1, 2, \dots$  [10]. In contrast to the field multipole moments defined at infinity,  $M_n$  and  $J_n$  are the source

multipole moments. We shall not discuss these moments here in any detail, except to say that in the vacuum case, the moments are essentially obtained by decomposing  $\Psi_2$  at  $\Delta$  into spherical harmonics based on preferred coordinates adapted to the axial symmetry. As at infinity, the Kerr horizon corresponds to a specific choice of these multipoles, but due to the non-linearity of general relativity, the field and source moments will not generally agree. See e.g. [61, 47, 45, 59] for some applications of these multipole moments.

## 4.5 The near horizon geometry

In a number of astrophysical applications where black holes play a role, it is not directly the horizon which is involved but rather the spacetime in the vicinity of the black hole. An especially interesting example of relevance to gravitational wave observations is the case of a binary system consisting of a stellar mass black hole or star orbiting around a much larger black hole (see e.g. [1] for a review of the astrophysics of such systems). As the small particle orbits the large black hole, it effectively “maps” the spacetime in the vicinity of the large black hole, much as the motion of satellites around Earth enables us to map Earth’s gravitational potential and therefore its shape. If carried out to sufficient precision, a measurement of gravitational waves from such a system would enable us to determine the gravitational field in the vicinity of the large black hole (see e.g. [58, 44]). One expects that the black hole is well approximated by a Kerr spacetime and we can seek to measure deviations from it thereby testing an important prediction of general relativity. Typical studies on this subject assume the black hole to be Kerr, which is entirely reasonable to a very good approximation (nearby stars or other matter fields might distort the black hole somewhat, but this is expected to be a small effect). However, for mathematical purposes, we could pose the question from a different viewpoint: If we specify the intrinsic geometry of the horizon, then to what extent is the near horizon spacetime determined by the horizon geometry? If we assume the large black hole to be in equilibrium (an excellent approximation for the case we have just described), then it seems reasonable to model the black hole as an isolated horizon. So the question then is: Can we find solutions to the Einstein field equations which admit a generic isolated horizon as an inner boundary? If so, then what is the extra data (beyond the intrinsic horizon geometry) that needs to be specified? (A full solution to the problem would require us to go beyond isolated horizons and to consider small deviations from equilibrium, but we shall not discuss this generalization here).

It turns out that these questions can be clearly answered if we use the characteristic initial value formulation of Einstein’s equations where free data is specified on a set of intersecting null hyper-surfaces [31, 57, 32, 62]. Consider  $N$  dependent variables  $\psi_I (I = 1, \dots, N)$  on a spacetime manifold with coordinates  $x^a$ . We shall be concerned with hyperbolic first-order quasi-linear equations of the form

$$\sum_{J=1}^N A_{IJ}^a(x, \psi) \partial_a \psi_J + F_I(x, \psi) = 0. \quad (64)$$

In the standard Cauchy problem, one specifies the  $\psi_I$  at some initial time. A solution is then guaranteed to be unique and to exist at least locally in time. The characteristic formulation considers a pair of null surfaces  $\mathcal{N}_0$  and  $\mathcal{N}_1$  whose intersection is a co-dimension-2 spacelike surface  $S$ . It turns out to be possible to specify appropriate data on the null surfaces and on  $S$  such that the above system of equations is well posed and has a unique solution, at least locally near  $S$ .

In our case, the appropriate free data is specified on the horizon and on an outgoing past light cone originating from a cross section of the horizon. Such a construction in the context of

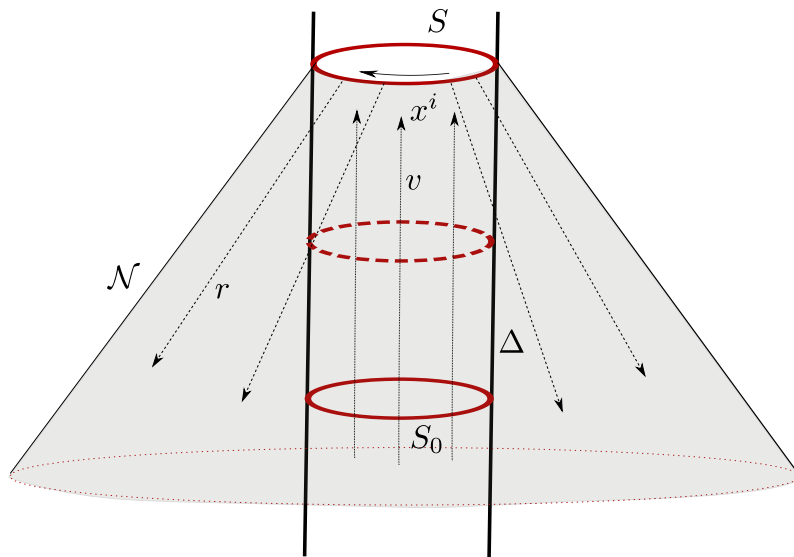


Figure 11: The near horizon coordinates. The isolated horizon is  $\Delta$  and the transverse null surface is  $\mathcal{N}$ . The affine parameter along the outgoing null geodesics on  $\mathcal{N}$  is  $r$ , and  $v$  is a coordinate along the null generators on  $\Delta$ , and  $x^i$  are coordinates on the cross-sections of  $\Delta$ .

isolated horizons was first studied by Lewandowski [51] who characterized the general solution of Einstein equations admitting an isolated horizon. This was worked out in detail in [49] which we follow here; similar results from a somewhat different perspective are discussed in [25]. The general scenario is sketched in Figure 11. We consider a portion of the horizon  $\Delta$  which is isolated, in the sense that no matter and/or radiation is falling into this portion of the horizon. For a cross-section  $S$ , the past-outgoing light cone is denoted by  $\mathcal{N}$ . The null generators of  $\Delta$  and  $\mathcal{N}$  are parameterized by  $v$  and  $r$  respectively;  $x^i$  are coordinates on  $S$ . This leads to a coordinate system  $(v, r, x^i)$  which is valid till the null geodesics on  $\mathcal{N}$  start to cross. The field equations are solved in a power series in  $r$  away from the horizon.

Let us now assume that the vacuum Einstein equations hold in a neighborhood of the horizon  $\Delta$ . Following [11] we introduce a coordinate system and null tetrad in the vicinity of  $\Delta$  analogous to the Bondi coordinates near null infinity. See Fig. 11. Choose a particular null normal  $\ell^a$  on  $\Delta$ . Let  $v$  be the affine parameter along  $\ell^a$  so that  $\ell^a \nabla_a v = 1$ . Let  $S_v$  denote the spheres of constant  $v$ . Introduce coordinates  $x^i$  ( $i = 2, 3$ ) on any one  $S_v$  (call this sphere  $S_0$ ) and require them to be constant along  $\ell^a$ :  $\ell^a \nabla_a x^i = 0$ ; this leads to a coordinate system  $(v, x^i)$  on  $\Delta$ . Let  $n^a$  be a future directed inward pointing null vector orthogonal to the  $S_v$  and normalized such that  $\ell \cdot n = -1$ . Extend  $n^a$  off  $\Delta$  geodesically, with  $r$  being an affine parameter along  $-n^a$ ; set  $r = 0$  at  $\Delta$ . This yields a family of null surfaces  $\mathcal{N}_v$  parameterized by  $v$  and orthogonal to the spheres  $S_v$ . Set  $(v, x^i)$  to be constant along the integral curves of  $n^a$  to obtain a coordinate system  $(v, r, x^i)$  in a neighborhood of  $\Delta$ . Choose a complex null vector  $m^a$  tangent to  $S_0$ . Lie drag  $m^a$  along  $\ell^a$ :

$$\mathcal{L}_\ell m^a = 0 \quad \text{on } \Delta. \quad (65)$$

We thus obtain a null tetrad  $(\ell, n, m, \bar{m})$  on  $\Delta$ . Finally, parallel transport  $\ell$  and  $m$  along  $-n^a$  to obtain a null tetrad in the neighborhood of  $\Delta$ . This construction is fixed up to the choice

of the  $x^i$  and  $m^a$  on an initial cross-section  $S_0$ . We are allowed to perform an arbitrary spin transformation  $m \rightarrow e^{i\psi} m$  on  $S_0$ .

With the Bondi-like coordinate system in hand, we can now in principle use the coordinate basis vectors in the  $(v, r, x^i)$  coordinates to construct an arbitrary null-tetrad near the horizon. The evolution equations for the component functions of the null tetrad will follow from the above construction. Let us start with  $n_a$  and  $n^a$ . We have the family of null surfaces  $\mathcal{N}_v$  parameterized by  $v$ ;  $n_a$  is normal to the  $\mathcal{N}_v$ , and  $r$  is an affine parameter along  $-n^a$ . This implies that we can choose

$$n_a = -\partial_a v \quad \text{and} \quad n^a \nabla_a := \Delta = -\frac{\partial}{\partial r}. \quad (66)$$

To satisfy the inner-product relations  $\ell^a n_a = -1$  and  $m^a n_a = 0$ , the other basis vectors must be of the form:

$$\ell^a \nabla_a := D = \frac{\partial}{\partial v} + U \frac{\partial}{\partial r} + X^i \frac{\partial}{\partial x^i}, \quad m^a \nabla_a := \delta = \Omega \frac{\partial}{\partial r} + \xi^i \frac{\partial}{\partial x^i}. \quad (67)$$

The frame functions  $U, X^i$  are real while  $\Omega, \xi^i$  are complex. We wish to now specialize to the case when  $\ell^a$  is a null normal of  $\Delta$  so that the null tetrad is adapted to the horizon. Since  $\partial_v$  is tangent to the null generators of  $\Delta$ , this clearly requires that  $U, X^i$  must vanish on the horizon. Similarly, we want  $m^a$  to be tangent to the spheres  $S_v$  at the horizon, so  $\Omega$  should also vanish on  $\Delta$ . Thus,  $U, X^i, \Omega$  are all  $\mathcal{O}(r)$  functions.

To expand the metric in powers of  $r$ , we start with the frame fields, and the radial frame equations derived from the commutation relations. The strategy is the same as for the spin coefficients. The radial equations give us the first radial derivatives by substituting the horizon values on the right hand side, and taking higher derivatives leads to the higher order terms. The calculations are straightforward and lead to the following expansions:

$$\left\{ \begin{array}{l} U = r\tilde{\kappa} + r^2 \left( 2|\pi^{(0)}|^2 + \text{Re}[\Psi_2^{(0)}] \right) + \mathcal{O}(r^3), \end{array} \right. \quad (68a)$$

$$\left\{ \begin{array}{l} \Omega = r\bar{\pi}^{(0)} + r^2 \left( \mu^{(0)}\bar{\pi}^{(0)} + \bar{\lambda}^{(0)}\pi^{(0)} + \frac{1}{2}\bar{\Psi}_3^{(0)} \right) + \mathcal{O}(r^3), \end{array} \right. \quad (68b)$$

$$\left\{ \begin{array}{l} X^i = \bar{\Omega}\xi_{(0)}^i + \Omega\bar{\xi}_{(0)}^i + \mathcal{O}(r^3), \end{array} \right. \quad (68c)$$

$$\left\{ \begin{array}{l} \xi^i = \left[ 1 + r\mu^{(0)} + r^2 \left( (\mu^{(0)})^2 + |\lambda^{(0)}|^2 \right) \right] \xi_{(0)}^i \\ \quad + \left[ r\bar{\lambda}^{(0)} + r^2 \left( 2\mu^{(0)}\bar{\lambda}^{(0)} + \frac{1}{2}\bar{\Psi}_4^{(0)} \right) \right] \bar{\xi}_{(0)}^i + \mathcal{O}(r^3). \end{array} \right. \quad (68d)$$

The contravariant metric is seen to be given in terms of the frame fields as follows:

$$\left\{ \begin{array}{l} g^{rr} = 2(U + |\Omega|^2), \quad g^{vr} = 1, \end{array} \right. \quad (69a)$$

$$\left\{ \begin{array}{l} g^{ri} = X^i + \bar{\Omega}\xi^i + \Omega\bar{\xi}^i, \quad g^{ij} = \xi^i\bar{\xi}^j + \bar{\xi}^i\xi^j. \end{array} \right. \quad (69b)$$

The null co-tetrad can be calculated easily up to  $\mathcal{O}(r^2)$ :

$$\left\{ \begin{array}{l} n = -dv, \end{array} \right. \quad (70)$$

$$\left\{ \begin{array}{l} \ell = dr - \left( \tilde{\kappa}r + \text{Re}[\Psi_2^{(0)}]r^2 \right) dv - \left( \pi^{(0)}r + \frac{1}{2}\Psi_3^{(0)}r^2 \right) \xi_{(0)}^i dx^i - \left( \bar{\pi}^{(0)}r + \frac{1}{2}\bar{\Psi}_3^{(0)}r^2 \right) \bar{\xi}_{(0)}^i dx^i, \end{array} \right. \quad (71)$$

$$\left\{ \begin{array}{l} m = - \left( \bar{\pi}^{(0)}r + \frac{1}{2}\Psi_3^{(0)}r^2 \right) dv + (1 - \mu^{(0)}r)\xi_{(0)}^i dx^i - \left( \bar{\lambda}^{(0)}r + \frac{1}{2}\bar{\Psi}_4^{(0)}r^2 \right) \bar{\xi}_{(0)}^i dx^i. \end{array} \right. \quad (72)$$

Here  $\xi_i^{(0)}$  are defined by the relations  $\xi_i^{(0)}\xi_{(0)}^i = 0$  and  $\xi_i^{(0)}\bar{\xi}_{(0)}^i = 1$ ; it will be convenient to set  $m_a^{(0)} := \xi_i^{(0)}\partial_a x^i$ . In powers of  $r$ , the metric is:

$$g_{ab} = -2\ell_{(a}n_{b)} + 2m_{(a}\bar{m}_{b)} = g_{ab}^{(0)} + g_{ab}^{(1)}r + \frac{1}{2}g_{ab}^{(2)}r^2 + \dots, \quad (73)$$

where

$$g_{ab}^{(0)} = 2\partial_{(a}r\partial_{b)}v + 2m_{(a}^{(0)}\bar{m}_{b)}^{(0)}, \quad (74)$$

$$g_{ab}^{(1)} = -\left(2\bar{\kappa}\partial_{(a}v\partial_{b)}v + 4\pi^{(0)}m_{(a}^{(0)}\partial_{b)}v + 4\bar{\pi}^{(0)}\bar{m}_{(a}^{(0)}\partial_{b)}v + 4\mu^{(0)}m_{(a}^{(0)}\bar{m}_{b)}^{(0)} + 2\lambda^{(0)}m_{(a}^{(0)}m_{b)}^{(0)} + 2\bar{\lambda}^{(0)}\bar{m}_{(a}^{(0)}\bar{m}_{b)}^{(0)}\right), \quad (75)$$

$$g_{ab}^{(2)} = 4\left(|\pi^{(0)}|^2 - \text{Re}[\Psi_2^{(0)}]\right)\partial_{(a}v\partial_{b)}v + 4\left(\mu^{(0)}\pi^{(0)} + \lambda^{(0)}\bar{\pi}^{(0)} - \Psi_3^{(0)}\right)m_{(a}^{(0)}\partial_{b)}v + 4\left(\mu^{(0)}\bar{\pi}^{(0)} + \bar{\lambda}^{(0)}\pi^{(0)} - \bar{\Psi}_3^{(0)}\right)\bar{m}_{(a}^{(0)}\partial_{b)}v + 4\left((\mu^{(0)})^2 + |\lambda^{(0)}|^2\right)m_{(a}^{(0)}\bar{m}_{b)}^{(0)} + \left(4\mu^{(0)}\lambda^{(0)} - 2\Psi_4^{(0)}\right)m_{(a}^{(0)}m_{b)}^{(0)} + \left(4\mu^{(0)}\bar{\lambda}^{(0)} - 2\bar{\Psi}_4^{(0)}\right)\bar{m}_{(a}^{(0)}\bar{m}_{b)}^{(0)}. \quad (76)$$

Iterating this procedure to higher orders is, in principle, straightforward. This calculation provides a starting point for a number of ongoing work in applying isolated and quasi-local horizons to astrophysical situations.

## 4.6 Angular momentum, mass, and the first law for isolated horizons

The first law for black holes, and black hole thermodynamics in general, was developed by Bekenstein [20], and by Bardeen, Carter and Hawking [17] in 1973 in analogy with the laws of thermodynamics. The zeroth law says that the surface gravity is constant over the black hole horizon. We have already seen that this is true for a weakly isolated horizon: the surface gravity  $\kappa_\ell = \ell^a\omega_a$  is constant on  $\Delta$ . The main difference with the standard formulation for a globally stationary the surface gravity refers to the globally defined stationary Killing vector which is normalized to have unit norm at infinity. A weakly isolated horizon does not refer to any globally defined Killing vector. The standard formulation of the second law says that the area of the event horizon can never decrease in time. The area of a non-expanding horizon is constant, thus the second law is trivial in this context.

Let us now turn to the first law. The standard formulation for a stationary black hole is

$$\delta M = \frac{\kappa}{8\pi}\delta a + \Omega\delta J. \quad (77)$$

Here  $M$  is the mass measured at spatial infinity,  $\kappa$  is the surface gravity at the event horizon but using a vector field normalized at infinity,  $a$  is the area of the horizon,  $\Omega$  is the angular velocity at the horizon,  $J$  is the angular momentum at infinity. Electromagnetic fields can also be included and leads to additional terms This is reasonable when applied to a globally stationary spacetime, but clearly needs to be refined for a black hole in equilibrium locally in an otherwise dynamical spacetime. It turns out that it is possible to formulate the first law for isolated horizons using quantities defined only at the horizon, without reference to the behavior of fields at infinity [6, 7, 12, 8]. The set-up is a variational problem in a portion of spacetime bounded inside by an axisymmetric weakly isolated horizon  $(\Delta, [\ell^a])$  (the extension to multiple horizons is straightforward).

Before talking about the first law, we need to first have suitable notions of the horizon angular momentum and mass. We begin with angular momentum. Fix an axial symmetry  $\varphi^a$



at the horizon. This means that  $\varphi^a$  must preserve (i) the equivalence class  $[\ell^a]$  of null normals that is prescribed for the weakly isolated horizon, (ii) the intrinsic metric  $q_{ab}$  and (iii) the 1-form  $\omega_a$ . Furthermore,  $\varphi^a$  should commute with  $\ell^a$  and it should look like a rotational vector field in that it should have closed integral curves, an affine length of  $2\pi$ , and should vanish at exactly two null horizon generators. Consider then a rotational vector field  $\phi^a$  in spacetime such that at  $\Delta$  it is equal to the fixed symmetry:  $\phi^a|_{\Delta} = \varphi^a$ . At infinity, we require that it approach some fixed rotational symmetry of the asymptotic flat metric. We then need to find the Hamiltonian<sup>1</sup>  $H_\phi$  which generates motions along  $\phi^a$ . The Hamiltonian can be shown to reduce to integrals over the boundaries at the horizon and at infinity. The term at  $\Delta$  is identified with the angular momentum of  $\Delta$ :

$$J_\phi^\Delta = -\frac{1}{8\pi} \oint_S \varphi^a \omega_a{}^2 \epsilon. \quad (78)$$

Similarly, the notion of energy corresponds to time translations. Thus, we consider time evolution vector fields  $t^a$  on spacetime such that at the horizon, it approaches a general symmetry vector  $A\ell^a + \Omega\varphi^a$ . Here the coefficients  $A$  and  $\Omega$  are constants on  $\Delta$ , but are allowed to vary in phase space. The strategy is then again to compute the surface term at  $\Delta$  in the Hamiltonian  $H_t$  which generates motions along  $t^a$ , and the surface term at  $\Delta$  is to be identified as the energy  $E_t^\Delta$ . Surprisingly, it turns out that motions along  $t^a$  are not always Hamiltonian and in fact, the Hamiltonian exists if and only if

$$\delta E_t^\Delta = \frac{\kappa_t}{8\pi} \delta a_\Delta + \Omega_t \delta J_\Delta. \quad (79)$$

This is just the first law, and a vector field  $t^a$  is said to be *permissible* if the first law for  $E_t^\Delta$  is satisfied. If the first law is satisfied, it is easy to see that  $\kappa_t, \Omega_t$  can depend only on the horizon quantities  $(a_\Delta, J_\Delta)$ , and must satisfy integrability condition

$$\frac{\partial \kappa_t(a_\Delta, J_\Delta)}{\partial J_\Delta} = \frac{\partial \Omega(a_\Delta, J_\Delta)}{\partial a_\Delta}. \quad (80)$$

This ensures that the right-hand-side of Eq. (79) can be integrated to yield an exact variation, and to thus have a well defined  $E_t^\Delta$ .

A preferred choice of  $t^a$  at the horizon can be obtained by choosing  $\kappa(a_\Delta, J_\Delta)$  and  $\Omega(a_\Delta, J_\Delta)$  to have the same functional dependence on  $(a_\Delta, J_\Delta)$  as in the Kerr spacetime:

$$\kappa = \frac{R_\Delta^4 - 4J_\Delta^2}{2R_\Delta^3 \sqrt{R_\Delta^4 + 4J_\Delta^2}}, \quad \Omega = \frac{2J_\Delta}{R_\Delta \sqrt{R_\Delta^4 + 4J_\Delta^2}}. \quad (81)$$

This leads to the horizon mass:

$$M_\Delta = \frac{1}{2R_\Delta} \sqrt{R_\Delta^4 + 4J_\Delta^2}. \quad (82)$$

Finally, we note that  $J_\phi^\Delta$  is independent of the choice of cross-section  $S$  and even though it requires a weakly isolated horizon to carry out the Hamiltonian computation, the formula of Eq. (78) itself is well defined even on a non-expanding horizon. If a cross-section  $S$  of  $\Delta$  is contained within a spatial hyper-surface  $\Sigma$ , and if  $\hat{r}^a$  is the unit spacelike normal to  $S$  in  $\Sigma$  and  $K_{ab}$  is the extrinsic curvature of  $\Sigma$ , then we can rewrite  $J_\phi^\Delta$  as

$$J_\phi^\Delta = \frac{1}{8\pi} \oint_S K_{ab} \varphi^a \hat{r}^b{}^2 \epsilon. \quad (83)$$

---

<sup>1</sup>Recall that in a phase space, a Hamiltonian is responsible for generating time evolution via the Poisson bracket. Thus, for any function  $F$  in a phase space,  $\dot{F} = \{H, F\}$ . In the present case, the phase space consists of gravitational (and other) fields which satisfy the appropriate boundary conditions.

This is particularly convenient in numerical relativity where one routinely located MTSs on spatial Cauchy surfaces, and would like to use them to characterize the properties of a black hole in real time while the simulation is in progress [29]. The computation of angular momentum is a surface integral over the MTS and the mass is just an algebraic expression. These methods are now in common use in numerical simulations.

## 5 Dynamical horizons

### 5.1 The area increase law

The second law for event horizons states that the area of an event horizon can never decrease in time. This was first suggested by Bekenstein and is the starting point for associating the area of a black hole horizon with entropy. We have thus far not talked about the area increase law for quasi-local horizons except in the context of isolated horizons where it is essentially trivial. For a dynamical horizon, the area increase law follows easily from the fact that  $\Theta_{(n)} < 0$ . Let  $\mathcal{H}$  be a dynamical horizon and  $S$  a generic MTS on it. Let  $r^a$  be the spacelike unit normal to  $S$  within  $\mathcal{H}$ ; this is not to be confused with the unit normal  $\hat{r}^a$  to  $S$  which lies on a spatial hyper-surface intersecting  $\mathcal{H}$  as in Fig. 9. Let  $\tau^a$  be the unit-timelike vector normal to  $\mathcal{H}$ . We assume also that  $r^a$  points outwards, in the sense that if  $\hat{r}^a$  is the outward normal to  $S$  on a spatial hyper-surface  $\Sigma$ , then  $r^a \hat{r}_a > 0$ . Finally, let  $\mathcal{H}$  be bounded by the cross-sections  $S_1$  and  $S_2$ . Then, a suitable choice for the out- and in-going null normals to  $S$  are

$$\ell^a = \frac{\tau^a + r^a}{\sqrt{2}}, \quad \tau^a = \frac{\tau^a - r^a}{\sqrt{2}}. \quad (84)$$

Then, if  $q_{ab}$  is the intrinsic Riemannian metric on  $S$ :

$$\sqrt{2}q^{ab}\nabla_a r_b = q^{ab}\nabla_a(\ell^a - \tau^a) = \Theta_{(\ell)} - \Theta_{(n)} > 0. \quad (85)$$

Thus, the area element on  $S$  and thus its area increases along  $r^a$ . (Though we shall not pursue this further, one could imagine relaxing the requirement  $\Theta_{(n)} < 0$  by an average on  $S$  and still obtain the same result). This is the area increase law for dynamical horizons.

We can go further and ask whether it is possible to obtain a *physical process* version of the area increase law which relates the increase in area from an initial cross-section  $S_1$  to a later time  $S_2$  to the amount of energy or radiation falling into the black hole between  $S_1$  and  $S_2$ . An early result along these lines was proved by Hartle and Hawking in 1972 [40] for perturbations of the event horizon. We note however that such a law does not exist for event horizons in general. A case in point being the Vaidya solution which as we have seen, grows in flat space when nothing falls into the black hole. Let us then consider the area increase law on a dynamical horizon  $\mathcal{H}$ . Let us first consider angular momentum and the change in angular momentum from  $S_1$  to  $S_2$ .

Since  $\mathcal{H}$  is a spacelike hyper-surface we have, as discussed earlier, the induced metric  $h_{ab}$ , the associated derivative operator  $D_a$ , and the extrinsic curvature  $K_{ab}$ . As before, let  $\tau^a$  be the unit timelike normal to  $\mathcal{H}$  and let  $r^a$  be the unit spacelike normal to a cross-section  $S$  within  $\mathcal{H}$ . The Einstein equations then show that  $(h_{ab}, K_{ab})$  cannot be specified freely, but must satisfy the Hamiltonian and momentum constraint equations (see e.g. [65]). The momentum constraint is:

$$D_b(K^{ab} - Kh^{ab}) = 8\pi T^{bc}n_c h_b^a. \quad (86)$$

Contracting both sides with a rotational vector field  $\varphi^a$  and integrate by parts to obtain

$$\frac{1}{8\pi} \oint_{S_2} K_{ab} \varphi^a r^b d^2V - \frac{1}{8\pi} \oint_{S_1} K_{ab} \varphi^a r^b = \int_{\mathcal{H}} \left( T_{ab} \tau^a \varphi^b + \frac{1}{16\pi} P^{ab} \mathcal{L}_\varphi h_{ab} \right), \quad (87)$$

where  $P^{ab} = K^{ab} - Kh^{ab}$ . We then identify the angular momentum of a cross-section  $S$  as

$$J_S^{(\varphi)} = -\frac{1}{8\pi} \int_S K_{ab} \varphi^a r^b d^2V. \quad (88)$$

Eq. (87) is thus a *balance* law for angular momentum [14, 15]. It relates  $J_{S_2}^{(\varphi)} - J_{S_1}^{(\varphi)}$  with the gravitational and matter flux crossing the horizon between  $S_2$  and  $S_1$ . We note that if  $\varphi^a$  is a Killing vector of the metric  $h_{ab}$ , then the gravitational contribution vanishes identically.

A similar (but more involved calculation) leads to a balance law for the change in area, or rather for the area radius  $R$  defined as  $R = \sqrt{a/4\pi}$  [14, 15]:

$$\frac{R_2}{2} - \frac{R_1}{2} = \int_{\mathcal{H}} T_{ab} \tau^a \xi^b d^3V + \frac{1}{16\pi} \int_{\mathcal{H}} N_r (|\sigma|^2 + 2|\zeta|^2) d^3V. \quad (89)$$

Here  $|\sigma|^2 := \sigma_{ab} \sigma^{ab}$  with  $\sigma_{ab}$  being the shear of the outgoing null vector  $\ell^a = \tau^a + r^a$ ;  $|\zeta|^2 := \zeta_a \zeta^a$  where  $\zeta^a = h^{ab} r^c \nabla_c \ell_b$ ; and  $N_r := |D_a R D^a R|^{1/2}$ . Eq. (89) is the desired area balance law. Again the flux terms consist of a matter and gravitational contributions. The integrand in the gravitational part is manifestly local and non-negative, and the matter contribution is positive if the dominant energy condition holds. The gravitational contribution in fact vanishes in spherical symmetry as it should. Along similar lines, Jaramillo andourgoulhon obtained a second order differential equation for the area [37] which leads to a causal evolution of the area subject to initial conditions (the analogous evolution of the area of an event horizon [27] turns out to be teleological in the sense that it requires one to specify a boundary condition near future timelike infinity).

Let us conclude with few words about angular momentum. We have identified Eq. (88) with the angular momentum of a cross-section of the dynamical horizon, while earlier we had identified Eq. (83) with the angular momentum of a cross-section of an isolated horizon. It can be shown that when  $\varphi^a$  is a symmetry of the intrinsic metric, then the two agree. Recently, it was shown by Jaramillo et al [46], that for an axisymmetric MOTS which is stably outermost, and if the spacetime satisfies the dominant energy condition, then the angular momentum  $J$  defined as above, satisfies the inequality  $|J| \leq a/8\pi$  where  $a$  is the area of  $S$ . Here, axisymmetry is imposed only at  $S$  and not globally. This surprising result further validates the identification of Eq. (88) as the angular momentum.

## 5.2 Uniqueness results for dynamical horizons

In earlier sections, we have already discussed the location and time evolution of trapped and marginally trapped surfaces. We now discuss further results obtained by Ashtekar and Galloway [13] related to the issue of uniqueness of marginally trapped surfaces in the dynamical case.

The first result, proved in [13], concerns the uniqueness of the foliation of a dynamical horizon by marginally trapped surfaces. Let  $\mathcal{H}$  be a dynamical horizon foliated by a set marginally trapped surfaces  $S_t$  with  $t$  being a continuous real parameter taking values within an open interval. Let  $S$  be a *weakly* trapped surface in  $\mathcal{H}$ , i.e. both of its expansions are non-positive:  $\Theta_{(\ell)} \leq 0$ ,  $\Theta_{(n)} \leq 0$  (in particular,  $S$  could be a marginally trapped surface). Then  $S$  must in fact be a marginally trapped surface and must coincide with one of the  $S_t$ . This shows that the foliation of  $\mathcal{H}$  by the  $S_t$  must be unique. As a corollary, consider as in Fig. 9, a MTT generated by MTSs  $S_t$  which lie in spacelike surfaces  $\Sigma_t$ . This is a situation common in numerical relativity where one uses the  $\Sigma_t$  for time evolution, and one locates MTSs on them. If we were to use a different foliation, and in particular a particular spatial hyper-surface  $\Sigma'$  which does not coincide with any of the  $\Sigma_t$ . If the intersection  $\Sigma' \cap \mathcal{H}$  is not

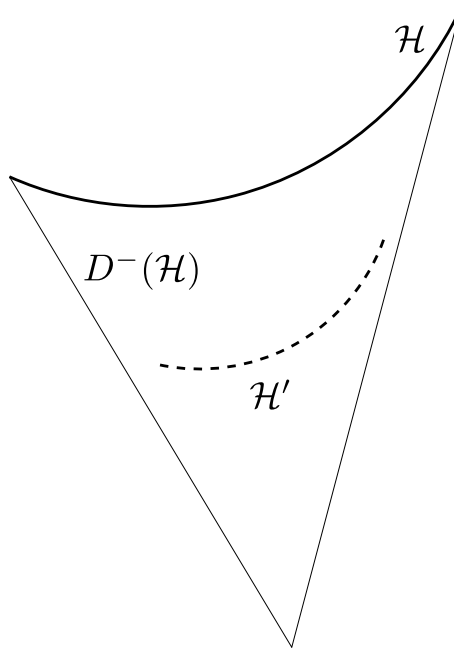


Figure 12: This situation is ruled out by the uniqueness results of Ashtekar and Galloway. If there is a dynamical horizon  $\mathcal{H}$ , then there cannot be another dynamical horizon  $\mathcal{H}'$  lying completely in the past domain of dependence  $D^-(\mathcal{H})$ .

one of the  $S_t$ , then it cannot be a marginally trapped surface. This is illustrated in Fig. 7 for the Vaidya spacetime. The intersection of the non-symmetric spatial hyper-surface with the spherically symmetric dynamical horizon is the red surface, and it is not a marginally (or weakly) trapped surface. Thus, if we had a different foliation  $\Sigma'_t$  and we locate MTSs on these spatial hyper-surfaces, then we would end up with a *different* dynamical horizon  $\mathcal{H}'$ . We note again the dramatic difference for an isolated horizon where every spherical cross-section is a marginally outer trapped surface.

The question then arises, how different can  $\mathcal{H}'$  be from  $\mathcal{H}$ . A partial answer is provided by the next result [13]: *There are no weakly trapped surfaces contained in the past domain of dependence  $D^-(\mathcal{H})$  (apart from those which make up  $\mathcal{H}$  itself)*<sup>2</sup>. In particular, this result rules out a dynamical horizon contained in  $D^-(\mathcal{H}) - \mathcal{H}$ . Once again, this result is illustrated by the Vaidya example discussed earlier in Fig. 4. The non-symmetric surface  $S$  in this figure is partly inside and partly outside the spherically symmetric dynamical horizon. More generally, weakly trapped surfaces lying partly inside  $D^-(\mathcal{H})$  are not ruled out.

## 6 Outlook

As discussed in the introduction, ever since the discover of the Schwarzschild solution almost a century ago, research in black holes has led to seminal developments in theoretical,

<sup>2</sup>The past domain of dependence  $D^-(\mathcal{H})$  is the set of spacetime points  $p$  such that every future causal curve from  $p$  intersects  $\mathcal{H}$

observational and computational physics. This includes the singularity theorems, black hole thermodynamics, the uniqueness theorems, the cosmic censorship hypothesis, black hole entropy calculations in various approaches to quantum gravity, the various astrophysical phenomena involving black holes, and the recent results from numerical relativity. The framework of quasi-local horizons, which takes trapped and marginally trapped surfaces as its starting point, provides a unified approach for studying various aspects of black hole physics. While we have only touched upon a few aspects and applications of this framework, the material presented in this chapter will hopefully motivate the reader to delve further into the subject. An important theme in this discussion is that to base our understanding of black holes on lessons from stationary cases can be misleading. Dynamical situations have some essentially different features and intuition from stationary examples can easily lead us astray. We have illustrated this by the Schwarzschild and Vaidya examples.

In this chapter we have introduced trapped surfaces and various kinds of quasi-local horizons through examples. The eventual goal of these studies (from a physics viewpoint) is to understand the properties of the surface of a black hole. We have discussed the inadequacy of event horizons for this purpose due to its teleological properties, and it is desirable to find a suitable replacement. Penrose's trapped surfaces and the boundary of the trapped region seem ideally suited for this task and lead naturally to the various definitions of quasi-local horizons. The simplest example is of course the Schwarzschild black hole. In this example, the boundary of the trapped region agrees with the event horizon, and both notions give rise to the same physical ideas. Difficulties arise however when we consider non-stationary black holes. We illustrated this through the imploding Vaidya spacetime. The intuitively obvious horizon, the analog of the  $r = 2M$  hyper-surface in Schwarzschild is a spherically symmetry dynamical horizon and it is separated from the event horizon. However, the non-spherically symmetric outer trapped surfaces extend up to the event horizon. To make matters more complicated, trapped surfaces do not extend all the way to the event horizon. We used these examples as motivations for general definitions and we reviewed some basic results regarding trapped surfaces and quasi-local horizons. We saw that marginally trapped surfaces are not as ill-behaved as one might think, and under physically reasonable conditions, they do evolve smoothly. The equilibrium case, described by isolated horizons is also of great interest. It covers a wide variety of situations where a black hole is in equilibrium in a dynamical spacetime and is the best understood quasi-local horizon. Finally, in the dynamical case, we saw that one can assign physical quantities such as mass, angular momentum and fluxes through dynamical horizons.

There are a number of topics that we have not discussed. In particular, we have not discussed the various applications of these notions in numerical relativity. Similarly, our discussion has been restricted to the classical world and we have not talked about e.g. the quantization of isolated horizons and the black hole entropy calculations. Even in the discussion of the mathematical properties of quasi-local horizons, we have discussed black hole multipole moments, symmetries, and inclusion of various kinds of matter fields only very briefly. Another significant omission is the discussion of black holes near equilibrium. Reviews of these topics can be found in e.g. [36, 24, 16]

We have seen that the outstanding question in this field is the non-uniqueness of dynamical horizons. We have discussed some restrictions on where dynamical horizons can be located. However, it is a fact that there are a multitude of smooth marginally trapped tubes and dynamical horizons in a general black hole spacetime, and there seems to be no obvious way of picking a preferred one. While there could be reasonable choices in specific examples, there does not seem to be any general solution to this problem. While one can get away with using event horizons in globally stationary spacetimes, choosing to live with event horizons in general is not an option because of its global properties. One could perhaps consider dealing with the

full set of dynamical horizons and marginally trapped tubes. Many of them are smooth one can study them individually; e.g. the dynamical horizon flux formulae apply to all dynamical horizons equally. However, if we wish to assign physical properties to the black hole such as mass, angular momentum, fluxes and higher multipoles, which one should we choose? We will generally get different results depending on our choice. The boundary of the trapped region could be a reasonable alternative, but as we have seen, it is generally not a marginally trapped tube itself. It is also not clear whether one can use this boundary to study, say, black hole thermodynamics and other physical phenomena that we believe are true for black holes and besides, this boundary also has a number of global properties and is difficult to locate (thus making it not better than event horizons in many regards). An interesting possibility, suggested by Bengtsson and Senovilla, is the *core* of the black hole region, i.e. the portion of the trapped region where all trapped surfaces penetrate. Removing the core would then completely eliminate all trapped surfaces. If it is indeed a proper subset of the trapped region, then is its boundary a dynamical horizon? There are indications that the region  $r \leq 2M(v)$  region of Vaidya is such a core, and its boundary is the spherically symmetric dynamical horizon. However the core is not unique and some cores are not spherically symmetric [23]. It is an interesting open question whether this idea can be developed further.

## Acknowledgment

I am grateful to Abhay Ashtekar for valuable discussions and suggestions.

## References

- [1] P. Amaro-Seoane, J. R. Gair, M. Freitag, M. Coleman Miller, I. Mandel, et al. Astrophysics, detection and science applications of intermediate- and extreme mass-ratio inspirals. *Class.Quant.Grav.*, 24:R113–R169, 2007.
- [2] L. Andersson, M. Mars, J. Metzger, and W. Simon. The Time evolution of marginally trapped surfaces. *Class.Quant.Grav.*, 26:085018, 2009.
- [3] L. Andersson, M. Mars, and W. Simon. Local existence of dynamical and trapping horizons. *Phys.Rev.Lett.*, 95:111102, 2005.
- [4] L. Andersson, M. Mars, and W. Simon. Stability of marginally outer trapped surfaces and existence of marginally outer trapped tubes. *Adv.Theor.Math.Phys.*, 12, 2008.
- [5] L. Andersson and J. Metzger. The Area of horizons and the trapped region. *Commun.Math.Phys.*, 290:941–972, 2009.
- [6] A. Ashtekar, C. Beetle, and S. Fairhurst. Isolated horizons: A generalization of black hole mechanics. *Class. Quant. Grav.*, 16:L1–L7, 1999.
- [7] A. Ashtekar, C. Beetle, and S. Fairhurst. Mechanics of Isolated Horizons. *Class. Quant. Grav.*, 17:253–298, 2000.
- [8] A. Ashtekar, C. Beetle, and J. Lewandowski. Mechanics of Rotating Isolated Horizons. *Phys. Rev.*, D64:044016, 2001.
- [9] A. Ashtekar, C. Beetle, and J. Lewandowski. Geometry of Generic Isolated Horizons. *Class. Quant. Grav.*, 19:1195–1225, 2002.
- [10] A. Ashtekar, J. Engle, T. Pawłowski, and C. Van Den Broeck. Multipole moments of isolated horizons. *Class. Quant. Grav.*, 21:2549–2570, 2004.

- [11] A. Ashtekar et al. Isolated horizons and their applications. *Phys. Rev. Lett.*, 85:3564–3567, 2000.
- [12] A. Ashtekar, S. Fairhurst, and B. Krishnan. Isolated horizons: Hamiltonian evolution and the first law. *Phys. Rev.*, D62:104025, 2000.
- [13] A. Ashtekar and G. J. Galloway. Some uniqueness results for dynamical horizons. *Adv. Theor. Math. Phys.*, 9:1–30, 2005.
- [14] A. Ashtekar and B. Krishnan. Dynamical horizons: Energy, angular momentum, fluxes and balance laws. *Phys. Rev. Lett.*, 89:261101, 2002.
- [15] A. Ashtekar and B. Krishnan. Dynamical horizons and their properties. *Phys. Rev.*, D68:104030, 2003.
- [16] A. Ashtekar and B. Krishnan. Isolated and dynamical horizons and their applications. *Living Rev. Rel.*, 7:10, 2004.
- [17] J. M. Bardeen, B. Carter, and S. W. Hawking. The Four laws of black hole mechanics. *Commun. Math. Phys.*, 31:161–170, 1973.
- [18] R. Beig and W. Simon. The stationary gravitational field near spacial infinity. *Gen. Rel. Grav.*, 12:1003–1013, 1980.
- [19] A. Bejancu and K. Duggal. *Lightlike submanifolds of semi-Riemannian manifolds and applications*. Kluwer Academic (Dordrecht and Boston, Mass.), 1996.
- [20] J. D. Bekenstein. Black holes and entropy. *Phys. Rev.*, D7:2333–2346, 1973.
- [21] I. Ben-Dov. Outer Trapped Surfaces in Vaidya Spacetimes. *Phys. Rev.*, D75:064007, 2007.
- [22] I. Bengtsson and J. M. M. Senovilla. A Note on trapped Surfaces in the Vaidya Solution. *Phys. Rev.*, D79:024027, 2009.
- [23] I. Bengtsson and J. M. M. Senovilla. The region with trapped surfaces in spherical symmetry, its core, and their boundaries. *Phys. Rev.*, D83:044012, 2011.
- [24] I. Booth. Black hole boundaries. *Can. J. Phys.*, 83:1073–1099, 2005.
- [25] I. Booth. Spacetime near isolated and dynamical trapping horizons. *Phys. Rev.*, D87:024008, 2013.
- [26] S. Chandrasekhar. *The mathematical theory of black holes*. Oxford Classic Texts in the Physical Sciences, 1985.
- [27] T. Damour. *Quelques propriétés mécaniques, électromagnétiques, thermodynamiques et quantiques des trous noirs*. PhD thesis, University of Paris, 1979.
- [28] P. Diener. A New general purpose event horizon finder for 3-D numerical space-times. *Class. Quant. Grav.*, 20:4901–4918, 2003.
- [29] O. Dreyer, B. Krishnan, D. Shoemaker, and E. Schnetter. Introduction to Isolated Horizons in Numerical Relativity. *Phys. Rev.*, D67:024018, 2003.
- [30] D. M. Eardley. Black hole boundary conditions and coordinate conditions. *Phys. Rev.*, D57:2299–2304, 1998.
- [31] H. Friedrich. On the Regular and the Asymptotic Characteristic Initial Value Problem for Einstein’s Vacuum Field Equations. *Proc. Roy. Soc. Lond.*, A375:169–184, 1981.
- [32] H. Friedrich and A. D. Rendall. The Cauchy problem for the Einstein equations. *Lect. Notes Phys.*, 540:127–224, 2000. Einstein’s Field Equations and their Physical Interpretation, ed. by B. G. Schmidt, Springer, Berlin, 2000.

- [33] R. P. Geroch. Multipole moments. II. Curved space. *J. Math. Phys.*, 11:2580–2588, 1970.
- [34] R. P. Geroch and J. B. Hartle. Distorted black holes. *J. Math. Phys.*, 23:680, 1982.
- [35] R. P. Geroch and G. Horowitz. Asymptotically simple does not imply asymptotically Minkowskian. *Phys.Rev.Lett.*, 40:203–206, 1978.
- [36] E.ourgoulhon and J. L. Jaramillo. A 3+1 perspective on null hypersurfaces and isolated horizons. *Phys. Rept.*, 423:159–294, 2006.
- [37] E.ourgoulhon and J. L. Jaramillo. Area evolution, bulk viscosity and entropy principles for dynamical horizons. *Phys. Rev.*, D74:087502, 2006.
- [38] R. O. Hansen. Multipole moments of stationary space-times. *J. Math. Phys.*, 15:46–52, 1974.
- [39] S. Hawking and G. Ellis. *The large scale structure of space-time*. Cambridge Monographs on Mathematical Physics, Cambridge University Press, 1973.
- [40] S. W. Hawking and J. B. Hartle. Energy and angular momentum flow into a black hole. *Commun. Math. Phys.*, 27:283–290, 1972.
- [41] S. Hayward. General laws of black hole dynamics. *Phys.Rev.*, D49:6467–6474, 1994.
- [42] S. Hayward and M. Kriele. Outer trapped surfaces and their apparent horizon. *J. Math. Phys.*, 38:1593, 1997.
- [43] S. A. Hayward. Spin coefficient form of the new laws of black hole dynamics. *Class. Quant. Grav.*, 11:3025–3036, 1994.
- [44] S. A. Hughes. Gravitational waves from extreme mass ratio inspirals: Challenges in mapping the space-time of massive, compact objects. *Class.Quant.Grav.*, 18:4067–4074, 2001.
- [45] J. L. Jaramillo, R. P. Macedo, P. Moesta, and L. Rezzolla. Black-hole horizons as probes of black-hole dynamics I: post-merger recoil in head-on collisions. *Phys.Rev.*, D85:084030, 2012.
- [46] J. L. Jaramillo, M. Reiris, and S. Dain. Black hole Area-Angular momentum inequality in non-vacuum spacetimes. *Phys.Rev.*, D84:121503, 2011.
- [47] M. Jasiulek. A new method to compute quasi-local spin and other invariants on marginally trapped surfaces. *Class. Quant. Grav.*, 26:245008, 2009.
- [48] A. Komar. Covariant conservation laws in general relativity. *Phys. Rev.*, 113:934, 1959.
- [49] B. Krishnan. The spacetime in the neighborhood of a general isolated black hole. *Class.Quant.Grav.*, 29:205006, 2012.
- [50] J. Lee. *Riemannian Manifolds: An Introduction to Curvature*. Graduate Texts in Mathematics, Springer, 1997.
- [51] J. Lewandowski. Spacetimes Admitting Isolated Horizons. *Class. Quant. Grav.*, 17:L53–L59, 2000.
- [52] E. Newman and R. Penrose. An Approach to gravitational radiation by a method of spin coefficients. *J. Math. Phys.*, 3:566–578, 1962.
- [53] E. Newman and T. Unti. Behavior of asymptotically flat empty space. *J. Math. Phys.*, 3:891–901, 1962.
- [54] R. Newman. Topology and stability of marginal 2-surfaces. *Class. and Quant. Grav.*, 4:277–290, 1987.



- [55] A. B. Nielsen, M. Jasiulek, B. Krishnan, and E. Schnetter. The Slicing dependence of non-spherically symmetric quasi-local horizons in Vaidya Spacetimes. *Phys.Rev.*, D83:124022, 2011.
- [56] R. Penrose and W. Rindler. *Spinors and Spacetime: 1. Two-Spinor Calculus and Relativistic Fields*. Cambridge, Uk: Univ. Pr. ( 1984) 458 P. ( Cambridge Monographs On Mathematical Physics), 1984.
- [57] A. D. Rendall. Reduction of the characteristic initial value problem to the cauchy problem and its applications to the einstein equations. *Proc. Roy. Soc. Lond.*, 427:221–239, 1990.
- [58] F. D. Ryan. Accuracy of estimating the multipole moments of a massive body from the gravitational waves of a binary inspiral. *Phys.Rev.*, D56:1845–1855, 1997.
- [59] M. Saijo. Dynamic black holes through gravitational collapse: Analysis of multipole moment of the curvatures on the horizon. *Phys.Rev.*, D83:124031, 2011.
- [60] E. Schnetter and B. Krishnan. Non-symmetric trapped surfaces in the Schwarzschild and Vaidya spacetimes. *Phys. Rev.*, D73:021502, 2006.
- [61] E. Schnetter, B. Krishnan, and F. Beyer. Introduction to dynamical horizons in numerical relativity. *Phys. Rev.*, D74:024028, 2006.
- [62] J. Stewart. *Advanced General Relativity*. Cambridge Monographs on Mathematical Physics, 1991.
- [63] J. Thornburg. Event and Apparent Horizon Finders for 3+1 Numerical Relativity. *Living Rev. Rel.*, 10:3, 2007.
- [64] P. Vaidya. The Gravitational Field of a Radiating Star. *Proc. Indian Acad. Sci.*, A33:264, 1951.
- [65] R. M. Wald. *General Relativity*. The University of Chicago Press, 1984.
- [66] R. M. Wald and V. Iyer. Trapped surfaces in the Schwarzschild geometry and cosmic censorship. *Phys.Rev.*, D44:3719–3722, 1991.